



**HAL**  
open science

## Degradable Glycopolyester-Like Nanoparticles by Radical Ring-Opening Polymerization

Théo Pesenti, Daniel Domingo-Lopez, Emilie Gillon, Nada Ibrahim, Samir Messaoudi, Anne Imberty, Julien Nicolas

► **To cite this version:**

Théo Pesenti, Daniel Domingo-Lopez, Emilie Gillon, Nada Ibrahim, Samir Messaoudi, et al.. Degradable Glycopolyester-Like Nanoparticles by Radical Ring-Opening Polymerization. *Biomacromolecules*, 2022, 23 (9), pp.4015-4028. 10.1021/acs.biomac.2c00851 . hal-03805407

**HAL Id: hal-03805407**

**<https://hal.science/hal-03805407>**

Submitted on 7 Oct 2022

**HAL** is a multi-disciplinary open access archive for the deposit and dissemination of scientific research documents, whether they are published or not. The documents may come from teaching and research institutions in France or abroad, or from public or private research centers.

L'archive ouverte pluridisciplinaire **HAL**, est destinée au dépôt et à la diffusion de documents scientifiques de niveau recherche, publiés ou non, émanant des établissements d'enseignement et de recherche français ou étrangers, des laboratoires publics ou privés.

# Degradable Glycopolyester-Like Nanoparticles by Radical Ring-Opening Polymerization

*Théo Pesenti,<sup>1</sup> Daniel Domingo-Lopez,<sup>1</sup> Emilie Gillon,<sup>2</sup> Nada Ibrahim,<sup>1</sup> Samir Messaoudi,<sup>3,\*</sup>  
Anne Imberty,<sup>2</sup> Julien Nicolas<sup>1,\*</sup>*

<sup>1</sup> Université Paris-Saclay, CNRS, Institut Galien Paris-Saclay, 92296 Châtenay-Malabry,  
France

<sup>2</sup> Université Grenoble Alpes, CNRS, CERMAV, 38000 Grenoble, France

<sup>3</sup> Université Paris-Saclay, CNRS, BioCIS, 92296 Châtenay-Malabry, France

\*To whom correspondence should be addressed.

Email: [samir.messaoudi@universite-paris-saclay.fr](mailto:samir.messaoudi@universite-paris-saclay.fr) (SM)

E-mail: [julien.nicolas@u-psud.fr](mailto:julien.nicolas@u-psud.fr) (JN)

## **Abstract**

A small library of degradable polyester-like glycopolymers was successfully prepared by the combination of radical ring-opening copolymerization of 2-methylene-1,3-dioxepane as a cyclic ketene acetal (CKA) with vinyl ether (VE) derivatives, and a Pd-catalyzed thioglycoconjugation. The resulting thioglycopolymers were formulated into self-stabilized thioglyconanoparticles which were stable up to 4 months and were enzymatically degraded. Nanoparticles and their degradation products exhibited a good cytocompatibility on two healthy cell lines. Interactions between thioglyconanoparticles and lectins were investigated and highlighted the presence of both specific carbohydrate/lectin interactions and non-specific hydrophobic interactions. Fluorescent thioglyconanoparticles were also prepared either by encapsulation of Nile red, or by the functionalization of the polymer backbone with rhodamine B. Such nanoparticles were used to prove the cell internalization of the thioglyconanoparticles by lung adenocarcinoma (A549) cells which underlined the great potential of P(CKA-co-VE) copolymers for biomedical applications

## 1. Introduction

Understanding the role of carbohydrates in cellular functions has opened new perspectives, especially in terms of studying their role in healthy living systems,<sup>1-3</sup> and using them as targets in designing therapeutic tools for many diseases (e.g., cancers<sup>4</sup>, bacterial<sup>5-6</sup> or viral infections<sup>7-11</sup>). Carbohydrates can be advantageously used in the development of nanoscale systems for biomedical applications,<sup>12-16</sup> as they can confer advanced properties such as active targeting of specific diseased tissues, prevention of pathogen adhesion, or improvement of pharmacokinetics and pharmacodynamics.<sup>17-18</sup> In addition to the clinical importance of glycoengineering of therapeutic proteins,<sup>17-18</sup> synthetic glycopolymers appear as promising systems with great potential in nanomedicine. For instance, Sandostatin LAR® is composed of glucose-*star*-poly(lactic-*co*-glycolic acid) (PLGA) microspheres loaded with octreotide, a peptide drug, able to achieve its sustained release for one month. It has been approved in 1998 for the treatment of acromegaly and severe diarrhea associated with certain types of cancers.<sup>19</sup>

Synthetic glycopolymers can be obtained by ring-opening polymerization (ROP) of lactones, cyclic carbonates or *N*-carboxyanhydrides, to give degradable polymer backbones functionalized with sugar molecules (Figure 1a).<sup>20-25</sup> Even if such polymerization techniques exhibit several advantages (e.g., biodegradable polymer backbones, industrially scalable<sup>26</sup>), they lack versatility and robustness to achieve more elaborated and diverse structures, which can be obtained much more easily by radical polymerization.<sup>27-29</sup> A wide range of vinyl glycopolymers based on (meth)acrylic, styrenic or acrylamide backbones have indeed been synthesized by conventional and reversible deactivation radical polymerization techniques.<sup>20, 25, 30</sup> This has been made possible due to the compatibility of radical polymerization with glycosidic moieties, the rather benign and versatile polymerization conditions (e.g., great variety of solvents, including water) and the possibility to finely tune the composition, architecture and functionalities of vinyl polymers. However, most glycopolymers synthesized by radical polymerization consist of a vinyl backbone (or at least one vinyl block), which prevents any form of degradation (Figure 1b). If biomedical applications are envisioned, their non-degradability can represent an important drawback since it can lead to the accumulation of foreign materials in the body and thus to potential toxicity.

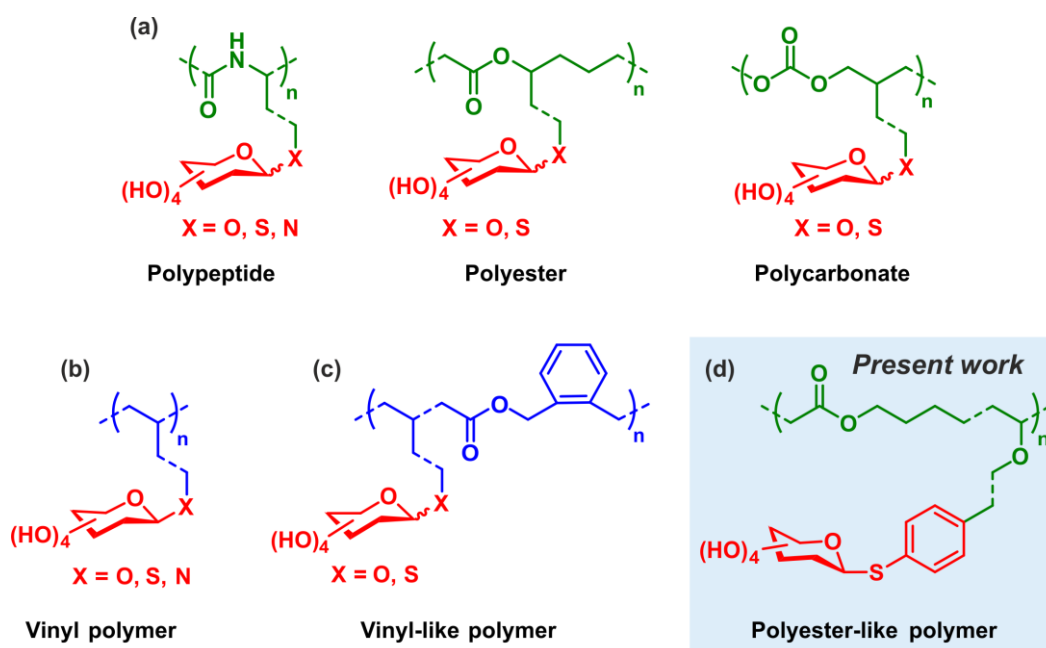


**Figure 1.** General structures of synthetic glycopolymers obtained by: (a) ring-opening polymerization (ROP) of *N*-carboxyanhydrides, lactones or cyclic carbonates; (b) radical polymerization of vinyl monomers; (c) radical ring-opening polymerization (rROP) of vinyl monomers and cyclic ketene acetals (here 5,6-benzo-2-methylene-1,3-dioxepane, BMDO and (d) rROP of vinyl ether and CKA (here 2-methylene-1,3-dioxepane, MDO).

Radical ring-opening polymerization (rROP) has recently gained renewed interest as an easy-to-implement approach of making degradable vinyl polymers,<sup>31-33</sup> in particular through a copolymerization approach. Among the monomers that can be copolymerized by rROP with traditional vinyl monomers, cyclic ketene acetals (CKAs), which are precursors of ester groups in the main chain, are undoubtedly the most used.<sup>31-33</sup> Not only can the resulting copolymers be degraded in small oligomers under various conditions (*e.g.*, hydrolytic degradation under alkaline or physiological conditions, enzymatic degradation), but they can also exhibit all advantages derived from the radical polymerization of vinyl monomers in terms of ease of synthesis, as well as structural and functional diversity.<sup>31-33</sup> While a wide range of vinyl monomers has been copolymerized with CKAs, only a very few studies have reported glycosylated CKA-based vinyl copolymers (Figure 1c).<sup>34-36</sup> For instance, Bai and co-workers copolymerized 1,2:3,4-di-*O*-isopropylidene-6-*O*-(2'-formyl-4'-vinylphenyl)-*D*-galactopyranose (IVDG) and 5,6-benzo-2-methylene-1,3-dioxepane (BMDO) by RAFT to produce P(IVDG-*co*-BMDO) copolymers that were self-assembled into glycosylated nanoparticles after deprotection of the hydroxyls groups of the sugar moieties.<sup>34</sup> Maynard and co-workers obtained trehalose-functionalized copolymers containing BMDO units *via* consecutive RAFT polymerization and thiol-ene post-functionalization to install trehalose moieties on the copolymer backbone.<sup>35</sup> By a combination of ROP

and rROP, Stenzel and co-workers chain-extended a polycaprolactone (PCL) macro RAFT agent with 1-O-acryloyl- $\beta$ -D-fructopyranose and BMDO to yield diblock copolymer micelles with a PCL core and a fructose-functionalized acrylic shell containing ester units.<sup>36</sup> In these systems, however, the CKA content was quite limited due to unfavorable reactivity ratios between CKAs and (meth)acrylic esters, and the resulting copolymers are more segmentable copolymers than fully degradable polyester-like copolymers. In addition, the hydrolytic degradation of CKA-containing copolymers obtained from (meth)acrylic esters is known to be very slow and their enzymatic degradation is often incomplete due to the hydrophobicity of the BMDO units which prevents efficient access of the enzyme to the ester groups.<sup>31-32</sup>

Herein, in order to overcome these limitations, we present a facile synthetic route to glycopolyester-like copolymers by rROP, which exhibit more than 90 % of PCL units (Figure 1d) and lead to complete enzymatic degradation. Our approach is based on a simple combination of a recently-developed copolymerization system between CKA and VEs,<sup>37-38</sup> allowing functional PCL-like copolymers to be obtained by a radical mechanism, and a Pd-catalyzed thioglycoconjugation methodology that operates under mild conditions.<sup>12, 39</sup> The resulting thioglycosylated copolymers were then formulated into self-stabilized nanoparticles (*i.e.*, without any surfactant) that showed: (i) interaction with the bacterial lectin LecA, a tetrameric galactose-binding lectin from *Pseudomonas aeruginosa* bacterium;<sup>40-41</sup> (ii) good cytocompatibility on two healthy cell lines (HUVEC and J774.A1); (iii) the possibility of being made fluorescent, either *via* encapsulation of Nile red as a model fluorescent dye, or *via* grafting of Rhodamine B moieties by the “*grafting through*” approach and (iv) successful internalization by lung adenocarcinoma (A549) cells.

## 2. Experimental part

### 2.1. Materials

All reagents and solvents were used as received. Methacryloxyethyl thiocarbonyl rhodamine B (RhoMA) was purchased from Polyscience. Lipase B *Candida antarctica* immobilized on Immunobead 150, recombinant from yeast (4584 U.g<sup>-1</sup>) was purchased from Sigma-Aldrich. LecA was produced from *E. coli* and purified as described elsewhere<sup>42</sup> All other reagents were purchased from Merck, TCI Chemicals or Thermo Fisher Scientific. 2-Methylene-1,3-dioxepane (MDO) was prepared by adapting

a previously published method, using the cyclic bromoacetal as intermediate.<sup>43</sup> The aminobiphenyl palladacycle precatalyst (Pd-G3-Xantphos), tetra-*O*-acetylated or unprotected 1-thio- $\beta$ -D-galactoses and tetra-*O*-acetylated or unprotected 1-thio- $\beta$ -D-glucoses were synthesized as previously described.<sup>39</sup> Diethylazobisisobutyrate (DEAB) was kindly supplied by Arkema. Deuterated solvents and anhydrous solvents were purchased from Eurisotop and Merck, respectively. All other solvents were purchased from Carlo Erba at the highest grade.

## 2.2. Analytical Methods

### 2.2.1. Nuclear Magnetic Resonance Spectroscopy (NMR)

NMR spectroscopy was performed in 5 mm diameter tubes in CDCl<sub>3</sub> or *d*<sub>6</sub>-DMSO at 25 °C. <sup>1</sup>H spectroscopy was performed on a Bruker Avance spectrometer at 300 MHz. The chemical shifts are reported in ppm ( $\delta$  units), and internal solvent signal ( $\delta = 7.26$  ppm for CDCl<sub>3</sub>,  $\delta = 2.5$  ppm for *d*<sub>6</sub>-DMSO) was used as a reference.

### 2.2.2. Size Exclusion Chromatography (SEC)

SEC of non-protic copolymers was performed on a Tosoh EcoSEC HLC-8320 with two columns from Agilent (PL-gel MIXED-D 300  $\times$  7.5 mm, beads diameter 5  $\mu$ m). Analyses were performed at 35°C in chloroform (HPLC grade) at a flow rate of 1 mL.min<sup>-1</sup>. Toluene (0.3 vol.%) was used as flow rate marker. Samples were filtered with a 0.22- $\mu$ m PTFE filter before analysis. The calibration curve was based on poly(methyl methacrylate) (PMMA) standards ( $M_p = 1\ 850\text{--}1\ 916\ 000$  g.mol<sup>-1</sup>) from Agilent. The EcoSEC Analysis software enabled the determination of the number-average molar mass ( $M_n$ ), the weight-average molar mass ( $M_w$ ) and the dispersity ( $\mathcal{D} = M_w/M_n$ ).

SEC of protic copolymers was performed on a Viscotek TDA/GPCmax from Malvern with two columns from Agilent (PL PolarGel-M, 300  $\times$  7.5 mm; bead diameter 8  $\mu$ m). Analyses were performed at 60 °C in DMSO (HPLC grade) with 10 mM LiBr (filtered over 0.22- $\mu$ m PTFE filters) at a flow rate of 0.7 mL.min<sup>-1</sup>. 2,6-Di-*tert*-butyl-4-methylphenol (BHT) (0.3 wt.%) was used as flow rate marker. Samples were filtered with a 0.22- $\mu$ m PTFE filter before analysis. The calibration curve was based on PMMA ( $M_p = 540\text{--}342\ 900$  g.mol<sup>-1</sup>) from Agilent. The OmniSEC software enabled the determination of  $M_n$ ,  $M_w$  and  $\mathcal{D}$ .

SEC of degraded copolymers was performed at 30 °C on a system equipped with two columns from Agilent (PL-gel MIXED-D 300  $\times$  7.5 mm, beads diameter 5  $\mu$ m), a differential refractive index

detector (Spectrasystem RI-150 from Thermo Electron Corp.), a scanning fluorescence detector (Waters 474) using chloroform with TFA (0.1 vol.%) as the eluent, and a Waters 515 HPLC Pump at a flow rate of 1 mL.min<sup>-1</sup>. Toluene (0.3 vol.%) was used as flow rate marker. Samples were filtered with a 0.22- $\mu$ m PTFE filter before analysis. The calibration curve was based on PMMA ( $M_p = 540\text{--}342\ 900$  g.mol<sup>-1</sup>) from Agilent. The OmniSEC software enabled the determination of  $M_n$ ,  $M_w$  and  $\mathcal{D}$ .

#### 2.2.3. Dynamic Light Scattering (DLS)

Nanoparticle diameter ( $D_z$ ) was measured by dynamic light scattering with a Nano ZS from Malvern with a detector angle of 173° (back scattering) at 25 °C. Samples were diluted 1:9 in the appropriate aqueous medium prior to measurement. Each measurement was performed in triplicate.

#### 2.2.4. $\zeta$ -potential measurement

$\zeta$ -potential was measured with a Nano ZS from Malvern at 25°C. Samples were diluted 1:9 in NaCl 1 mM prior to measurement. Each measurement was performed in triplicate.

#### 2.2.5. UV-visible spectroscopy

UV-vis absorbance spectra of samples were measured using a Lambda 25 UV/VIS spectrometer in a 350–800 nm range with a cell path length of 10 mm at 25 °C.

#### 2.2.6. Fluorescence spectroscopy

Emission fluorescence spectra of samples were measured at 25 °C using a spectrofluorimeter FP-750 (Jasco, Japan) with an excitation wavelength  $\lambda_{ex} = 488$  nm and an emission wavelengths in the 489–700 nm range.

### 2.3. Synthesis procedures

#### 2.3.1. Synthesis of the protected monomers

*Para-iodoaryl vinyl ether (IArVE)*. To a solution of 4-iodobenzoic acid (5 g, 0.02 mol, 1 equiv.) and DMAP (0.240 g, 2.00 mmol, 0.1 equiv.), was added anhydrous dichloromethane (DCM, 80 mL) under stirring at 0 °C, followed by degassing under argon atmosphere for 30 min and addition of ethylene glycol vinyl ether (3.60 mL, 0.04 mol, 2 equiv.). A solution of DCC (4.56 g, 0.02 mol, 1.1 equiv.) and anhydrous DCM (20 mL) was prepared under argon atmosphere and added dropwise to the reaction mixture at 0 °C under magnetic stirring for 20 min. After the addition was completed, the reaction mixture was warmed up to 30 °C and stirred for 24 h. A white solid appeared which was then filtered

off, followed by evaporation of the solvent under vacuum. The crude mixture was solubilized in DCM, adsorbed onto celite and purified by chromatographic column (cyclohexane:EtOAc 9:1, v:v). Combined fractions were evaporated under vacuum to yield IArVE as a white powder with 68 % yield (4.32 g, 13.60 mmol).

*Para-iodoaryl diethylene glycol vinyl ether (IArDEGVE)*. IArDEGVE was obtained using the same protocol, but ethylene glycol vinyl ether was replaced by diethylene glycol vinyl ether with the following amounts: 4-iodobenzoic acid (5 g, 20 mmol, 1 equiv.), DMAP (0.23 g, 1.9 mmol, 0.1 equiv.), diethylene glycol vinyl ether (6 mL, 44 mmol, 2.2 equiv.), DCC (4.77 g, 23 mmol, 1.1 equiv.). Purification was performed by chromatographic column (cyclohexane to cyclohexane:EtOAc 92:8 v/v). Yield: 55 % (4 g, 11 mmol).

*Tetra-acetylated thiogalactose vinyl ether ((AcO)<sub>4</sub>GalVE)*. In a 50-mL round-bottom flask, IArVE (503 mg, 1.58 mmol, 1 equiv.), tetra-acetylated 1-thio-β-D-galactopyranose (691 mg, 1.90 mmol, 1.2 equiv.), Pd-G3-Xantphos (31 mg, 0.03 mmol, 0.02 equiv.) and anhydrous THF (20 mL) were introduced. The resulting yellow mixture was degassed by Argon bubbling for 30 min under magnetic stirring. Then, triethylamine (700 μL, 5 mmol, 3 equiv.) was added. The mixture changed from yellow to orange/brown that evidenced the activation of the precatalyst and initiation of the reaction. The mixture was left at room temperature for 2 h until a solid is formed. 5 mL of MeOH was added to quench the reaction: the mixture became red without any solid. Solvents were evaporated under vacuum. The crude was solubilized in DCM, adsorbed onto celite and purified by chromatographic column (cyclohexane to cyclohexane:EtOAc 7:3, v/v). Combined fractions were evaporated under high vacuum in order to produce (AcO)<sub>4</sub>GalVE as an orange solid with 82 % yield (720 mg, 1.30 mmol). <sup>1</sup>H NMR (300 MHz, CDCl<sub>3</sub>): δ 4.80 (d, *J* = 9.9 Hz, *H*<sub>anomeric, g</sub><sup>\*</sup>)

*Tetra-acetylated thioglucose vinyl ether ((AcO)<sub>4</sub>GlcVE)*. (AcO)<sub>4</sub>GlcVE monomer was obtained following the above-mentioned protocol by using tetra-acetylated 1-thio-β-D-glucopyranose: IArVE (436 mg, 1.37 mmol, 1 equiv.), tetra-acetylated 1-thio-β-D-glucopyranose (600 mg, 1.65 mmol, 1.2 equiv.), Pd-G3-Xantphos (27 mg, 0.03 mmol, 0.02 equiv.) and triethylamine (600 μL, 4.31 mmol, 3 equiv.). Yield: 47 % (420 mg, 0.8 mmol). <sup>1</sup>H NMR (300 MHz, CDCl<sub>3</sub>): δ 4.82 (d, *J* = 10.2 Hz, *H*<sub>anomeric, g</sub><sup>\*</sup>)

*Tetra-acetylated thiogalactose diethylene glycol vinyl ether ((AcO)<sub>4</sub>GalDEGVE)*. (AcO)<sub>4</sub>GalDEGVE monomer was obtained following the above-mentioned protocol replacing IArVE

monomer by IArDEGVE: IArDEGVE (654 mg, 1.8 mmol, 1 equiv.), tetra-acetylated 1-thio- $\beta$ -D-galactopyranose (745 mg, 2.05, 1.1 equiv.), Pd-G3-Xantphos (37 mg, 0.04 mmol, 0.02 equiv.) and triethylamine (800  $\mu$ L, 5.75 mmol, 3 equiv.). Yield: 33 % (353 mg, 0.6 mmol).  $^1\text{H}$  NMR (300 MHz,  $\text{CDCl}_3$ ):  $\delta$  4.82 (d,  $J = 9.9$  Hz,  $H_{\text{anomeric, i}^*}$ )

### 2.3.2. Synthesis of protected thioglycopolymers by the “grafting through” approach

**P1-AcOGal.** In a 7-mL vial fitted with a rubber septum,  $(\text{AcO})_4\text{GalVE}$  (197 mg, 0.36 mmol), MDO (775 mg, 6.79 mmol,  $f_{\text{MDO},0} = 0.95$ ) and DEAB (36 mg, 0.14 mmol) were introduced. The mixture was degassed by Argon bubbling under magnetic stirring at r.t. for 30 min. The vial was immersed in a preheated oil bath at 90  $^\circ\text{C}$  under 300-rpm stirring for 24 h. The copolymer was purified by 3 precipitations in 50 mL of cold MeOH immersed in a NaCl iced water bath. For each precipitation, the pellet was recovered, and the supernatant was centrifuged at 10 000 rpm for 15 min. All pellets were combined to give a yellowish oil (370 mg).  $^1\text{H}$  NMR (300 MHz,  $\text{CDCl}_3$ ):  $\delta$  4.87 (d,  $J = 9.9$  Hz,  $H_{\text{anomeric, i}^*}$ )

**P2-AcOGal.** The same protocol as for **P1-AcOGal** was performed with  $f_{\text{MDO},0} = 0.88$  and the following amounts:  $(\text{AcO})_4\text{GalVE}$  (311 mg, 0.56 mmol), MDO (473 mg, 4.1 mmol) and DEAB (24 mg, 0.09 mmol). Purification of the copolymer was performed by 5 precipitations in 50 mL of a MeOH:H<sub>2</sub>O (9:1 v/v) mixture immersed in a NaCl iced water bath. A yellowish oil was obtained (111 mg).  $^1\text{H}$  NMR (300 MHz,  $\text{CDCl}_3$ ):  $\delta$  4.86 (d,  $J = 9.9$  Hz,  $H_{\text{anomeric, i}^*}$ )

**P3-AcOGal.** The same protocol as for **P1-AcOGal** was performed by using  $(\text{AcO})_4\text{GalDEGVE}$  and with the following amounts: MDO (665 mg, 5.83 mmol,  $f_{\text{MDO},0} = 0.95$ ),  $(\text{AcO})_4\text{GalDEGVE}$  (184 mg, 0.31 mmol) and DEAB (32 mg, 0.12 mmol). A yellowish oil was obtained (220 mg).  $^1\text{H}$  NMR (300 MHz,  $\text{CDCl}_3$ ):  $\delta$  4.84 (d,  $J = 9.9$  Hz,  $H_{\text{anomeric, k}^*}$ )

**P4-AcOGlc.** The same protocol as for **P1-AcOGal** was performed by using  $(\text{AcO})_4\text{GlcVE}$  and with the following amounts: MDO (796 mg, 6.97 mmol,  $f_{\text{MDO},0} = 0.95$ ),  $(\text{AcO})_4\text{GlcVE}$  (204 mg, 0.37 mmol) and DEAB (44 mg, 0.17 mmol). A yellowish oil was obtained (355 mg).  $^1\text{H}$  NMR (300 MHz,  $\text{CDCl}_3$ ):  $\delta$  4.86 (d,  $J = 10.2$  Hz,  $H_{\text{anomeric, i}^*}$ )

**Rho-P1-AcOGal.** The same protocol as for **P1-AcOGal** was performed by adding RhoMA in the comonomer feed and with the following amounts: MDO (900 mg, 7.89 mmol,  $f_{\text{MDO},0} = 0.95$ ),  $(\text{AcO})_4\text{GalVE}$  (228 mg, 0.41 mmol), RhoMA (5.5 mg, 8  $\mu$ mol) and DEAB (43 mg, 0.17 mmol).  $^1\text{H}$  NMR (300 MHz,  $\text{CDCl}_3$ ):  $\delta$  4.87 (d,  $J = 9.6$  Hz,  $H_{\text{anomeric, i}^*}$ )

**Rho-P4-AcOGlc.** The same protocol as for **P4-AcOGlc** was performed by adding RhoMA in the comonomer feed and with the following amounts: MDO (431 mg, 3.8 mmol,  $f_{\text{MDO},0} = 0.95$ ), (AcO)<sub>4</sub>GlcVE (110 mg, 0.2 mmol), RhoMA (3 mg, 5  $\mu\text{mol}$ ) and DEAB (19 mg, 0.08 mmol). <sup>1</sup>H NMR (300 MHz, CDCl<sub>3</sub>):  $\delta$  4.86 (d,  $J = 10.2$  Hz,  $H_{\text{anomeric, i}^*}$ )

### 2.3.3. Deprotection of the thioglycopolymers

In a 50-mL round-bottom flask fitted with a rubber septum, **P1-AcOGal** (350 mg, 0.15 mmol of (AcO)<sub>4</sub>GalVE unit), anhydrous THF (21.5 mL) and a magnetic stirring bar were introduced. The resulting homogenous yellowish liquid mixture was degassed using Argon bubbling under magnetic stirring for 30 min at 0 °C. Hydrazine monohydrate (282  $\mu\text{L}$ , 5.81 mmol) was added, followed by degassing under Argon bubbling for another 15 min. The flask was then immersed in a preheated oil bath at 30 °C for 24 h. Acetone (20 mL) was added, and the resulting cloudy crude became homogenous and yellowish upon acetone addition. Solvents were partially evaporated using a rotary evaporator before dialysis against acetone for 48 h (MWCO = 1 kDa, Biotech RC Spectra/Por®). Solvents were evaporated under high vacuum to obtain a yellowish oil (180 mg). <sup>1</sup>H NMR (300 MHz, *d*<sub>6</sub>-DMSO):  $\delta$  4.76 (d,  $J = 9.9$  Hz,  $H_{\text{anomeric, i}^*}$ )

The same protocol was performed for the other thioglycopolymers, with the following amounts and results: **P2-AcOGal** [copolymer (98 mg), yellowish oil (53 mg)]; **P3-AcOGal** [copolymer (157 mg), yellowish oil (81 mg)]; **P4-AcOGal** [copolymer (165 mg), yellowish oil (101 mg)]; **Rho-P1-AcOGal** [copolymer (53 mg), pink oil (27 mg)] and **Rho-P4-AcOGlc** [copolymer (178 mg), pink oil (103 mg)].

### 2.3.4. Synthesis of P(MDO-co-IArVE) copolymers

**P5-IAr.** In a 7-mL vial, MDO (585 mg, 5.12 mmol,  $f_{\text{MDO},0} = 0.95$ ), IArVE (87 mg, 0.27 mmol) and DEAB (27 mg, 0.10 mmol) were introduced. The mixture was degassed by argon bubbling for 30 min. Then, the mixture was immersed in a preheated oil bath at 90 °C and kept under stirring for 24 h. The copolymer was purified by 3 precipitations in cold *n*-heptane. For each precipitation, the pellet was recovered, and the supernatant was centrifuged at 10 000 rpm for 15 min. All pellets were combined to give a grayish viscous solid (152 mg).

**P6-IAr.** The same procedure as for **P5-IAr** was performed with  $f_{\text{MDO},0} = 0.90$  and the following amounts: MDO (530 mg, 4.64 mmol), IArVE (166 mg, 0.52 mmol) and DEAB (33 mg, 0.13 mmol). A grayish viscous solid was obtained (120 mg).

### 2.3.5. Synthesis of the thioglycopolymers by the “grafting to” approach

**P5-Gal. P5-IAr** (340 mg, 0.15 mmol of IArVE unit, 1 equiv.) and 1-thio- $\beta$ -D-galactopyranose (88 mg, 0.45 mmol, 3 equiv.) were dissolved in a mixture of THF (2 mL) and the minimum amount of Milli-Q water needed to dissolve the thiosugar partner. The reaction mixture was heated up to 50°C, stirred and degassed by Argon bubbling atmosphere for 15 min. A solution of Pd-G3-Xantphos precatalyst (10 mg, 0.01 mmol, 0.07 equiv) in THF (0.5 mL) was prepared and degassed. 10  $\mu$ L (0.3 eq, excess) of triethylamine was added on the precatalyst in order to activate it. The resulting mixture was transferred to the reaction mixture. The reaction was performed at 50 °C, under stirring and an inert atmosphere until completion (4 h, as determined by  $^1\text{H}$  NMR). The formation of an orange suspension was observed. 1 mL of DMSO was then added and the resulting yellow-orange liquid was purified by dialysis in THF:H<sub>2</sub>O (8:2, v/v) for 7 days (MWCO = 3.5 kDa, Biotech RC Spectra/Por®). The dialyzed sample was evaporated under high vacuum and freeze-dried for 2 days in order to produce an orange/brown viscous solid (126 mg). In order to purify **P5-Gal** from residual catalyst traces, **P5-Gal** (92 mg) was solubilized in 10 mL of a 1 vol.% of 3-mercaptopropionic acid (MCPA)<sup>44</sup> in a THF:H<sub>2</sub>O (8:2, v/v) mixture. After 30 min under magnetic stirring at 37 °C, the crude was dialyzed against THF:H<sub>2</sub>O (8:2, v/v) for 4 days and then against THF for 2 days. An orange oil was obtained (85 mg).  $^1\text{H}$  NMR (300 MHz, *d*<sub>6</sub>-DMSO):  $\delta$  4.75 (d,  $J$  = 9.9 Hz,  $H_{\text{anomeric, i}^*}$ )

**P6-Gal.** The same procedure was followed by adapting the reactants quantities and the nature of the sugar: **P6-IAr** (250 mg, 0.20 mmol IArVE), 1-thio- $\beta$ -D-galactopyranose (119 mg, 0.60 mmol) and Pd-G3-Xantphos (7 mg, 7.38  $\mu$ mol).  $^1\text{H}$  NMR (300 MHz, *d*<sub>6</sub>-DMSO):  $\delta$  4.75 (d,  $J$  = 9.3 Hz,  $H_{\text{anomeric, i}^*}$ )

**P5-Glc.** The same procedure was followed by adapting the reactants quantities and the nature of the sugar: **P5-IAr** (183 mg, 0.08 mmol IArVE), 1-thio- $\beta$ -D-glucopyranose (57 mg, 0.24 mmol) and Pd-G3-Xantphos (5 mg, 5.27  $\mu$ mol).  $^1\text{H}$  NMR (300 MHz, *d*<sub>6</sub>-DMSO):  $\delta$  4.79 (d,  $J$  = 9.0 Hz,  $H_{\text{anomeric, i}^*}$ )

## 2.4. Nanoparticle preparation

*Nanoprecipitation.* 2 mg of copolymer was dissolved in 670  $\mu$ L of THF. In a 7-mL vial, this solution was added dropwise to 2 mL of Milli-Q water or of an aqueous mixture of the surfactant (Table 3) under stirring (800 rpm). THF was then evaporated at 35 °C using a rotary evaporator for 1 h. Water was also evaporated in order to obtain the targeted concentration (1 or 5 mg.mL<sup>-1</sup>).

*Emulsion-solvent evaporation.* In a 7-mL vial, 2 mg of copolymer was dissolved in 400  $\mu$ L of dichloromethane. Sodium cholate aqueous solution (1 wt.% in Milli-Q water) was then introduced. The

resulting biphasic mixture was vortexed for 1 min and then sonicated in ice (Biorblock Scientific Vibra-Cell 75041, 45 s, 30 %). Organic solvent was evaporated at room temperature for 3 h under magnetic stirring.

Nanoparticle suspensions were characterized by DLS and  $\zeta$ -potential measurements. For stability study, the different samples were kept at room temperature under ambient light without any stirring.

## 2.5. Isothermal titration calorimetry (ITC)

Recombinant lyophilized LecA was dissolved in water in the presence of 100  $\mu$ M CaCl<sub>2</sub> and degassed. The LecA concentration was determined by measuring the optical density (Nanodrop) by using a theoretical absorbance extinction coefficient of 27 960 M<sup>-1</sup>.cm<sup>-1</sup>. The nanoparticles were diluted in the same solution and degassed. Reverse ITC experiments (nanoparticles in the cell) were performed at 25 °C, with a VP-ITC MicroCalorimeter from MicroCal Incorporated. Titration was performed with 10  $\mu$ L injections of LecA solution (1.74 mM) in the 1.466 mL cell with the nanoparticle solution ([glycoside] = 0.1 mM) every 300 s. Data were fitted with MicroCal PEAQ ITC analysis software according to standard procedures. Fitted data yielded the stoichiometry ( $n$ ), the association constant ( $K_a$ ) and the enthalpy of binding ( $\Delta H$ ). Other thermodynamic parameters (i.e., changes in free energy,  $\Delta G$ , and entropy,  $\Delta S$ ) were calculated from the equation  $\Delta G = \Delta H - T\Delta S = RT \ln K_a$ , in which  $T$  is the absolute temperature and  $R = 8.314 \text{ J.mol}^{-1}.\text{K}^{-1}$ . Two independent titrations were performed for each type of nanoparticles tested.

## 2.6. Enzymatic degradation

In a 20-mL vial, 2 mL of nanoparticle suspension (5 mg.mL<sup>-1</sup>) was diluted with 2 mL of phosphate buffer (25 mM, pH 7.2). 87 mg of *C. antarctica* Lipase B (4584 U.g<sup>-1</sup>) was then added to obtain 100 U.mL<sup>-1</sup>. After incubation at 37 °C (1 h, 125-rpm orbital shaking), the reaction medium was freeze-dried and then solubilized in CHCl<sub>3</sub>/TFA (0.1 vol.%). Enzymes and salts were removed by filtration over 0.22- $\mu$ m hydrophobic PTFE filter. CHCl<sub>3</sub> was evaporated under reduced pressure and the mixture was analyzed by SEC CHCl<sub>3</sub> (TFA 0.1 vol.%) (PMMA calibration).

## 2.7. Biological evaluation

*Cell Culture.* Human endothelial umbilical vein cells (HUVEC), murine macrophage monocytes (J774.A1) and adenocarcinomic human alveolar basal epithelial (A549) cells were maintained as recommended. HUVEC cells were grown in Dulbeccos's modified Eagle's medium (DMEM)-high glucose supplemented with 10% fetal bovine serum (FBS), penicillin ( $100 \text{ U.mL}^{-1}$ ) and streptomycin ( $100 \text{ U.mL}^{-1}$ ). J774.A1 and A549 cells were grown in Roswell Park Memorial Institute medium (RPMI) 1640 supplemented with 10 % FBS, penicillin ( $100 \text{ U.mL}^{-1}$ ) and streptomycin ( $100 \text{ U.mL}^{-1}$ ). Cells were maintained in a humid atmosphere at  $37 \text{ }^\circ\text{C}$  with 5 %  $\text{CO}_2$ .

*Cytotoxicity Study.* *In vitro* cytotoxicity of the nanoparticles and their degradation products was evaluated on the two healthy cell lines using 3-[4,5-dimethylthiazol-2-yl]-3,5-diphenyltetrazolium bromide (MTT) assay. Cells were seeded in 100  $\mu\text{L}$  of growth medium ( $2 \times 10^4 \text{ cells.mL}^{-1}$  for HUVEC,  $1.5 \times 10^4 \text{ cells.mL}^{-1}$  for J774.A1) in 96-well plates and incubated for 24 h. After appropriate dilutions in growth medium, 100  $\mu\text{L}$  of nanoparticles or degradation products mixtures was added on the cells and incubated for 72 h. After incubation, 20  $\mu\text{L}$  of MTT solution ( $5 \text{ mg.mL}^{-1}$  in PBS) was added to each well. The plates were incubated 1 h at  $37 \text{ }^\circ\text{C}$  and the medium was removed. 200  $\mu\text{L}$  of DMSO was then added to each well to dissolve the precipitates. Absorbance was measured at 570 nm using a plate reader (Metertech  $\Sigma$  960, Fisher Bioblock, Illkirch, France). The percentage of surviving cells was calculated as the absorbance ratio of treated cells to untreated cells. All experiments, set up in sextuplicate, were performed at least 3 times with at least 2 different batches of nanoparticles or degradation products, to determine means and standard deviations (SD).

*Confocal microscopy and cellular uptake.* A549 cells were seeded in 2 mL of growth medium ( $1.9 \times 10^5 \text{ cells.mL}^{-1}$ ) in a 6-well plate with a coverslip (0.17 thick, 25 mm diameter) in each well and incubated for 24 h. 2 mL of a fluorescent nanoparticles diluted in growth medium ( $0.1 \text{ mg.mL}^{-1}$ ) was added. The plate was incubated at  $37 \text{ }^\circ\text{C}$  with 5 %  $\text{CO}_2$ . At  $t = 20 \text{ min}$  and 2 h, the coverslip was set up in a microscopy cell chamber (Attolfluor Chamber). 500  $\mu\text{L}$  of calcein-AM ( $3 \mu\text{M}$  in phosphate buffer saline) was added. The coverslip was incubated for 10 min, and then the calcein-AM mixture was removed. Cells were washed 3 times with 500  $\mu\text{L}$  of growth medium and imaged by confocal laser scanning microscopy (Zeiss).

*Nile red (NR) encapsulation.* 2 mg of the copolymer was dissolved in 670 mg of a NR solution ( $0.06 \mu\text{g.mg}^{-1}$  in THF). In a 7-mL vial, this orange organic phase was introduced dropwise into 2 mL of Milli-Q water. The resulting intense dark purple mixture was evaporated using a rotary evaporator ( $35 \text{ }^\circ\text{C}$ , P

= 50 mbar, 1 h). The resulting magenta homogenous mixture was filtered over a 0.45- $\mu$ m PVDF syringe-filter. UV absorption and fluorescence measurements were then performed. NR-loaded nanoparticles were freeze-dried for 24 h. The dark purple polymer ( $m_{\text{copolymer}} + m_{\text{NR}}$ ) was solubilized in a known amount of THF. UV absorption was measured in order to determine encapsulated NR ( $m_{\text{encaps.NR}}$ ) according to a calibration (NR in THF, calibration curve:  $A(\lambda_{\text{max}} = 528 \text{ nm}) = 119.05 [\text{NR}]_{\mu\text{g}/\text{mg}} + 0.0297$ ,  $R^2 = 0.9978$ ). NR loading was determined according to the following:  $\text{NR (wt.\%)} = 100 \times [m_{\text{encaps.NR}} / (m_{\text{copolymer}} + m_{\text{NR}})]$ .

### 3. Results and Discussion

#### 3.1. Overall synthetic strategy

The copolymerization of MDO with VE was selected to achieve degradable vinyl thioglycopolymers. This nearly ideal copolymerization system allows the synthesis of PCL-like backbones due to the possibility of achieving very high fractions of MDO units ( $F_{\text{MDO}} \geq 0.9$ ) in the resulting P(CKA-co-VE) copolymer,<sup>37-38</sup> while leaving the possibility of functionalizing VE moieties.

The flexibility of radical polymerization offers two different synthetic routes to produce degradable P(CKA-co-VE) thioglycopolymers: (i) the “grafting to” approach, which consists in grafting thiosugar moieties onto a preformed degradable iodo-P(MDO-co-VE) backbone and (ii) the “grafting through” approach, which relies on the free-radical copolymerization between MDO and thiosugar-functionalized VE derivatives (Figure 2). Some of us recently reported an efficient Buchwald-Hartwig-Migita cross-coupling method allowing the selective introduction of glycosyl thiols to various iodoaryles,<sup>39</sup> nucleic acids<sup>45</sup> and peptides.<sup>12, 46</sup> The C-S bond formation was achieved under mild and biocompatible conditions by using the Pd-G3-Xantphos palladacycle pre-catalyst (Figure 2a), in the presence of triethylamine in an aqueous solvent.<sup>39</sup> Thus, we envisioned herein that this ligation strategy may be adapted to install thiosugar derivatives onto: (i) IArVE monomers (“grafting through” approach, Figure 2b, Path A) or (ii) P(MDO-co-IArVE) copolymers (“grafting to” approach, Figure 2b, Path B). If successful, this approach would provide not only an easy access to thioglycopolymers with original properties, but also open a new way for a broad array of biological applications with stables S-glycopolymers under biological conditions. Moreover, aromatic aglycon resulted in higher affinity

ligand for LecA,<sup>47-48</sup> and 1-thiogalactosides are more resistant to the metabolic hydrolysis under biological conditions.<sup>49</sup>

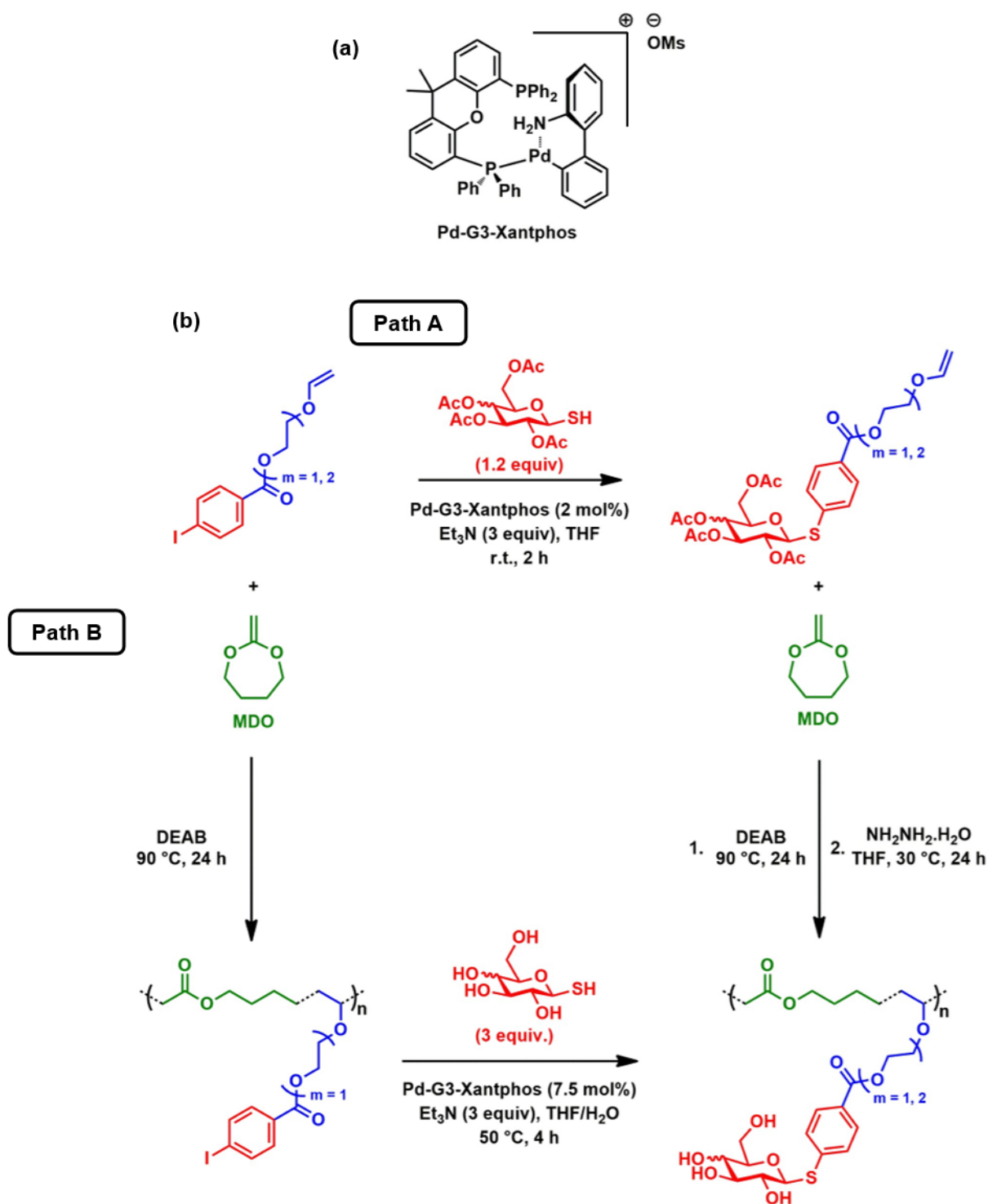


**Figure 2.** (a) Structure of the Pd-G3-Xantphos palladacycle precatalyst. (b) Synthesis of degradable vinyl thioglycopolymers by: (Path A) Pd-catalyzed coupling of protected 1-thiosugars to iodoaryl vinyl ether (IARVE) catalyzed by Pd-G3-Xantphos, followed by free-radical copolymerization of 2-methylene-1,3-dioxepane (MDO) and sugar-functionalized VE (“grafting through” approach) and (Path B) free-radical copolymerization of MDO and IARVE followed by grafting of 1-thiosugars catalyzed by Pd-G3-Xantphos (“grafting to” approach).

### 3.2. Copolymer synthesis

Both synthetic routes start with the synthesis of IArVE, which was obtained by DCC/DMAP coupling between ethylene glycol vinyl ether (EGVE) and 4-iodobenzoic acid, with a 68% yield (Figure S1).

For the “grafting through” approach, IArVE was reacted with tetra-acetylated 1-thiogalactose under Pd-catalyzed coupling by using Pd-G3-Xantphos (2 mol %) at room temperature for 2 h, to give the corresponding tetra-acetylated galactose VE monomer ((AcO)<sub>4</sub>GalVE) in a good yield (82 %) (Figure S2). Note that the P(MDO-co-GalVE) copolymer cannot be obtained by direct copolymerization using unprotected GalVE due to side reactions between MDO and the hydroxyl groups of the sugar nucleus.<sup>31</sup> Copolymerizations of (AcO)<sub>4</sub>GalVE and MDO ( $f_{\text{MDO},0} = 0.88$  or  $0.95$ ) were then performed in bulk at 90 °C for 24 h with DEAB as the initiator (**P1-AcOGal** and **P2-AcOGal**, Table 1, Figure 2, S3 and S5). The higher the  $f_{\text{VE},0}$ , the lower the MDO conversion, but the VE fractions in the resulting P(MDO-co-(AcO)<sub>4</sub>GalVE) copolymer were in line with the initial feed ratio ( $F_{\text{VE}} \sim f_{\text{VE},0}$ ), in agreement with a nearly ideal copolymerization process. Dispersities of the copolymers were mainly high, which are consistent with a free-radical polymerization process.

**Table 1.** Macromolecular characteristics of the degradable thioglycopolymers synthesized by the “grafting through” approach.

Ref	VE monomer	$f_{\text{VE},0}$	$F_{\text{VE}}^{\text{a}}$	Conv. MDO (%) <sup>a</sup>	$M_{\text{n}}$ (g.mol <sup>-1</sup> ) <sup>c</sup>	$\mathcal{D}^{\text{c}}$
<b>P1-AcOGal</b>	(AcO) <sub>4</sub> GalVE	0.05	0.05	66	14 300	2.0
<b>P2-AcOGal</b>	(AcO) <sub>4</sub> GalVE	0.12	0.13	31	7 500	1.7
<b>P3-AcOGal</b>	(AcO) <sub>4</sub> GalDEGVE	0.05	0.06	60	12 200	2.0
<b>P4-AcOGlc</b>	(AcO) <sub>4</sub> GlcVE	0.05	0.06	81	14 700	3.7
<b>P1-Gal</b>	GalVE	-	0.03	-	12 500	1.9
<b>P2-Gal</b>	GalVE	-	0.10	-	7 500	1.5
<b>P3-Gal</b>	GalDEGVE	-	0.04	-	11 500	1.6
<b>P4-Glc</b>	GlcVE	-	0.04	-	14 000	1.7

<sup>a</sup> Determined by <sup>1</sup>H NMR. <sup>b</sup> Determined by SEC in CHCl<sub>3</sub> (PMMA calibration). <sup>c</sup> Determined by SEC in DMSO with 10 mM LiBr (PMMA calibration).

Selective deprotection of the acetate protecting groups of the sugar unit in **P1-AcOGal** and **P2-AcOGal** was performed by hydrazine-mediated deacetylation<sup>50-51</sup> at 30 °C for 24 h. This method led to removal of acetyl groups without affecting the polyester backbone as shown by <sup>1</sup>H NMR in CDCl<sub>3</sub>,

which confirmed the synthesis of the targeted structures (**P1-Gal** and **P2-Gal**, Table 1, Figure 3a, 3b and S4-5). For instance, CH<sub>3</sub> acetyl protons at  $\delta = 1.9\text{--}2.1$  ppm disappeared while aromatic protons at  $\delta = 7.5$  and 8 ppm remained. Glycosidic proton signals at  $\delta = 4.8\text{--}5.5$  ppm also shifted to  $\delta \sim 4$  ppm upon deacetylation and overlapped with the polyester proton signals. Interestingly, when <sup>1</sup>H NMR was performed in d<sub>6</sub>-DMSO, glycosidic proton signals were present in the  $\delta = 4.2\text{--}5.3$  ppm region (Figure 3b). As evidenced by SEC, the thioglycopolymers exhibited a slight shift in *M<sub>n</sub>* towards lower values upon deprotection, while maintaining their molar mass distribution (Figure 3c). This confirmed the absence of degradation of the thioglycopolymer backbone during the deprotection step. However, VE contents were slightly affected, which could be attributed to some cleavage of the ester side groups, although the determination of such small amounts may be subject to imprecision.

To demonstrate the versatility of the synthesis pathway, it has then been successfully adapted to the synthesis of thioglycopolymers with: (i) a longer linker via the use of tetracetylated galactose diethylene glycol vinyl ether ((AcO)<sub>4</sub>GalDEGVE, **P3-AcOGal**, **P3-Gal**, Table 1 Figure S6-10) and (ii) glucose moieties *via* the use of tetracetylated glucose vinyl ether ((AcO)<sub>4</sub>GlcVE, **P4-AcOGlc**, **P4-Glc**, Table 1, Figure S11-14). Similar molar masses (*M<sub>n</sub>* = 11 500–14 000 g·mol<sup>-1</sup>) and dispersities (*D* = 1.6–1.7) as **P1-Gal** were obtained. This small library of P(MDO-co-VE) thioglycopolymers will be used thereafter to study the impact of the linker, *F<sub>VE</sub>* and the sugar nature on the thioglycopolymer properties.

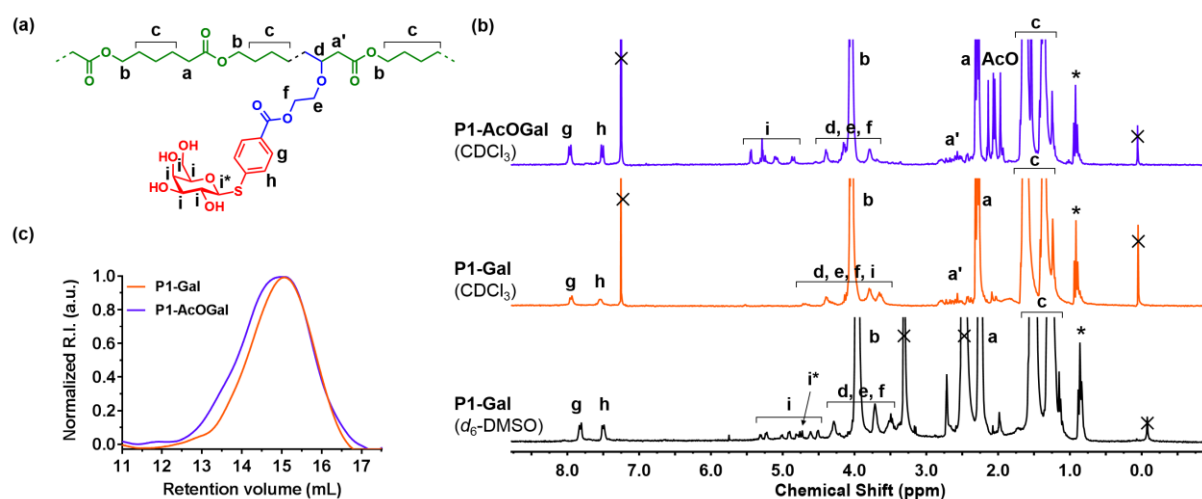


**Figure 3.** (a) Structure of **P1-Gal**. (b) <sup>1</sup>H NMR spectrum in the 0–8 ppm region of **P1-AcOGal** (CDCl<sub>3</sub>, purple), **P1-Gal** (CDCl<sub>3</sub>, orange) and **P1-Gal** (d<sub>6</sub>-DMSO, black). \* = CH<sub>3</sub> from MDO backbiting. (c) SEC chromatograms (DMSO with 10 mM LiBr) of **P1-AcOGal** (purple) and **P1-Gal** (orange).

For the “grafting to” approach, the copolymerizations between MDO and IArVE ( $f_{\text{IArVE},0} = 0.05$  and 0.10) were performed under the same conditions as for the “grafting through” strategy (**P5-IAr** and **P6-IAr**, Table 2, Figure 4 and S15-16). Although this resulted in lower MDO conversions and molar masses ( $M_n = 7\,000\text{--}9\,000\text{ g}\cdot\text{mol}^{-1}$ ), the expected structures were obtained with amounts of inserted IArVE units very close to the original feed ratios. These differences between the two synthetic methods could lie in potential side reactions between radicals and IAr moieties due to the well-known reactivity of the weak C-I bond towards radical species.<sup>52</sup>

**Table 2.** Macromolecular characteristics of the degradable thioglycopolymers synthesized by the “grafting to” approach.

Ref	VE monomer	$f_{\text{VE},0}$	$F_{\text{VE}}^a$	Conv. MDO (%) <sup>a</sup>	$M_n$ (g·mol <sup>-1</sup> )	$\mathcal{D}$
<b>P5-IAr</b>	IArVE	0.05	0.05	53	9 000 <sup>b</sup>	3.0 <sup>b</sup>
<b>P6-IAr</b>	IArVE	0.10	0.11	35	7 000 <sup>b</sup>	2.3 <sup>b</sup>
<b>P5-Gal</b>	GalVE	-	0.05	-	16 500 <sup>c</sup>	7.7 <sup>c</sup>
<b>P5-Glc</b>	GlcVE	-	0.06	-	12 200 <sup>c</sup>	4.3 <sup>c</sup>
<b>P6-Gal</b>	GalVE	-	0.10	-	10 200 <sup>c</sup>	2.8 <sup>c</sup>

<sup>a</sup> Determined by <sup>1</sup>H NMR. <sup>b</sup> Determined by SEC in CHCl<sub>3</sub> (PMMA calibration). <sup>c</sup> Determined by SEC in DMSO with 10 mM LiBr (PMMA calibration).

Interestingly, unlike the “grafting through” pathway, post-functionalization could be performed from unprotected 1-thiosugars, resulting in direct access to the desired thioglycopolymers (**P5-Gal**, **P5-Glc** and **P6-Gal**, Figure 4a and S17-20), providing optimization of the thioglycoconjugation conditions to ensure total efficiency (4 h, 50 °C, 7.5 mol % of Pd-G3-Xantphos). For instance, after purification by dialysis, <sup>1</sup>H NMR in CDCl<sub>3</sub> showed two doublets at 7.6 and 8.0 ppm for **P5-Gal** instead of a quadruplet at 7.8 ppm for **P5-IAr**, assessing the quantitative coupling of the 1-thiosugar onto the iodoaryl moieties (Figure 4b). As for the “grafting through” strategy, glycosidic proton signals were observed in the 4.4–5.3 ppm region by <sup>1</sup>H NMR in d<sub>6</sub>-DMSO.  $F_{\text{VE}}$  values were almost identical to the initial feed ratios for all thioglycopolymers (Table 2) and their  $M_n$  were similar to those obtained by the “grafting through” approach. However, their final dispersities were much higher due to the higher dispersity of the P(MDO-co-IArVE) parent copolymers.

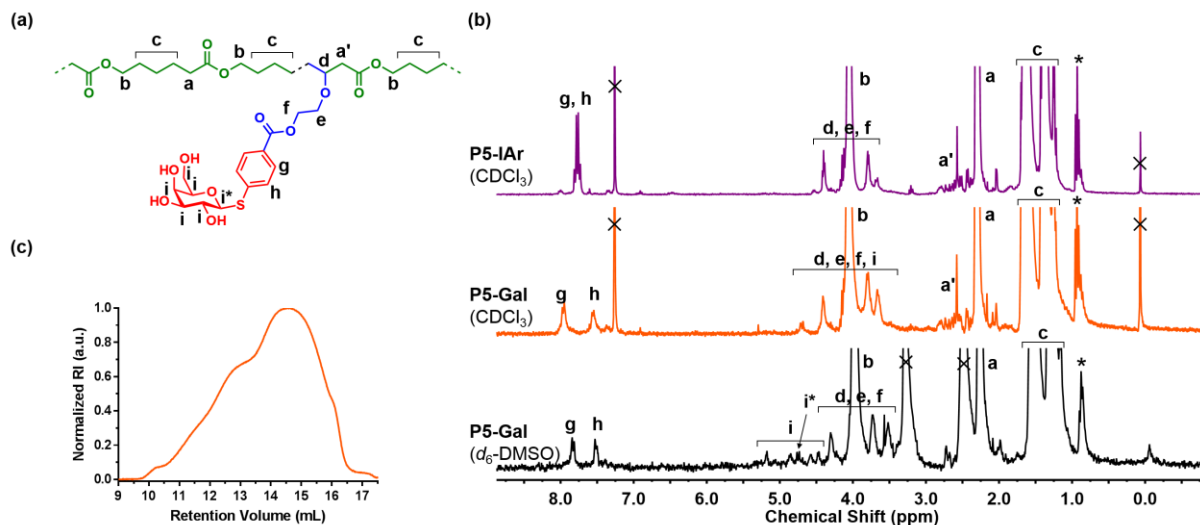


**Figure 4.** (a) Structure of **P5-Gal**. (b) <sup>1</sup>H NMR spectrum in the 0–8 ppm region of **P5-IAr** (CDCl<sub>3</sub>, blue), **P5-Gal** (CDCl<sub>3</sub>, green) and **P5-Gal** (d<sub>6</sub>-DMSO, black). \* = CH<sub>3</sub> from MDO backbiting. (c) SEC chromatogram (DMSO with 10 mM LiBr) of **P5-Gal**.

### 3.3. Formulation into degradable thioglycopolymer nanoparticles

The thioglycopolymers were then tested for their ability to be formulated into degradable thioglyconanoparticles by varying the formulation conditions, such as the formulation technique and the nature of the surfactant (Table 3). For **P1-Gal**, stable nanoparticles below 200 nm in size and with a low dispersity (PSD < 0.1) were obtained when nanoprecipitation was performed without surfactant or in the presence of Pluronic F68, or when emulsion-solvent evaporation was performed in the presence of sodium cholate. Although Pluronic F68 is not required to obtain stable thioglyconanoparticles, it represents a convenient way to impart a PEG-based coating to thioglyconanoparticles to induce stealth properties. Other surfactants were tested with the nanoprecipitation (sodium cholate, Tween 20 and PVA) but higher average diameters ( $D_z = 217\text{--}446$  nm) were obtained. Therefore, for the sake of simplicity, we focused on surfactant-free nanoparticles obtained by nanoprecipitation in the rest of the study.

**Table 3.** Colloidal characteristics of **P1-Gal**-based nanoparticles.

Technique	Surfactant		$D_z^a$ (nm)	PSD <sup>a</sup>
	Nature	Concentration (wt. %)		
Nanoprecipitation	-	-	121	0.05
	Pluronic F68	1	131	0.06
	Sodium Cholate	1	232	0.09
	Tween 20	1	446	0.09
	PVA	0.5	217	0.02
Emulsion-solvent evaporation	Sodium Cholate	1	90	0.08

<sup>a</sup> Determined by DLS.

Interestingly, stable and narrowly dispersed nanoparticles were obtained by surfactant-free nanoprecipitation for all types of thioglycopolymers (Table 4). However, additional purification of thioglycopolymers **P5-Gal** (obtained by the “*grafting to*” approach) by 3-mercaptopropionic acid (MCPA) for 30 min was required to remove the remaining catalyst which can coordinate the polyhydroxy functions<sup>39</sup> and cause colloidal instability. This led us to only consider thioglycopolymers obtained by the “*grafting through*” strategy for the rest of the study.

Varying the nature of the sugar and  $F_{VE}$  did not appear to have a significant effect on  $D_z$ , PSD or  $\zeta$ -potential, whereas a smaller size was obtained when increasing the length of the linker ( $D_z = 121$  nm for **NP1-Gal** vs. 76 nm for **NP3-Gal**). All thioglyconanoparticles remained stable for at least 4 months at room temperature with no significant change in size or dispersity (Figure S21).

**Table 4.** Colloidal characteristics of degradable thioglycopolymer nanoparticles obtained by surfactant-free nanoprecipitation.

Ref	Polymer	$D_z^a$ (nm)	PSD <sup>a</sup>	$\zeta$ -potential <sup>a</sup> (mV)
<b>NP1-Gal</b>	<b>P1-Gal</b>	121	0.05	-24
<b>NP2-Gal</b>	<b>P2-Gal</b>	108	0.01	-25
<b>NP3-Gal</b>	<b>P3-Gal</b>	76	0.07	-27
<b>NP4-Glc</b>	<b>P4-Glc</b>	87	0.05	-31
<b>NP5-Gal</b>	<b>P5-Gal<sup>b</sup></b>	167	0.09	-42

<sup>a</sup> Determined by DLS. <sup>b</sup> Washed with MCPA.

### 3.4. Nanoparticle-protein interactions

To investigate the accessibility of sugar moieties and to quantify the interactions between the thioglyconanoparticles and LecA, ITC analysis was performed (Figure 5). Addition of LecA (1.74 mM) in an aqueous suspension of **NP1-Gal** nanoparticles ([glycoside] = 0.1 mM) gave strong exothermic peaks while control experiment with water with 100  $\mu\text{M}$   $\text{CaCl}_2$  did not show significant heat of dilution (Figure 5a and 5b). This confirms the establishment of interactions between LecA and the nanoparticles, in agreement with the precipitation assay. However, the integration curve did not show a typical sigmoidal shape usually expected in the case of strong carbohydrate-lectin interactions. Although it should be taken very cautiously due to the non-sigmoidal shape, integration of the raw data led to a dissociation constant,  $K_d$ , in the millimolar range ( $K_d \sim 6 \text{ mM}$ ) which is not consistent with the strong avidity expected for LecA interaction with galacto-nanoparticles.<sup>53</sup>

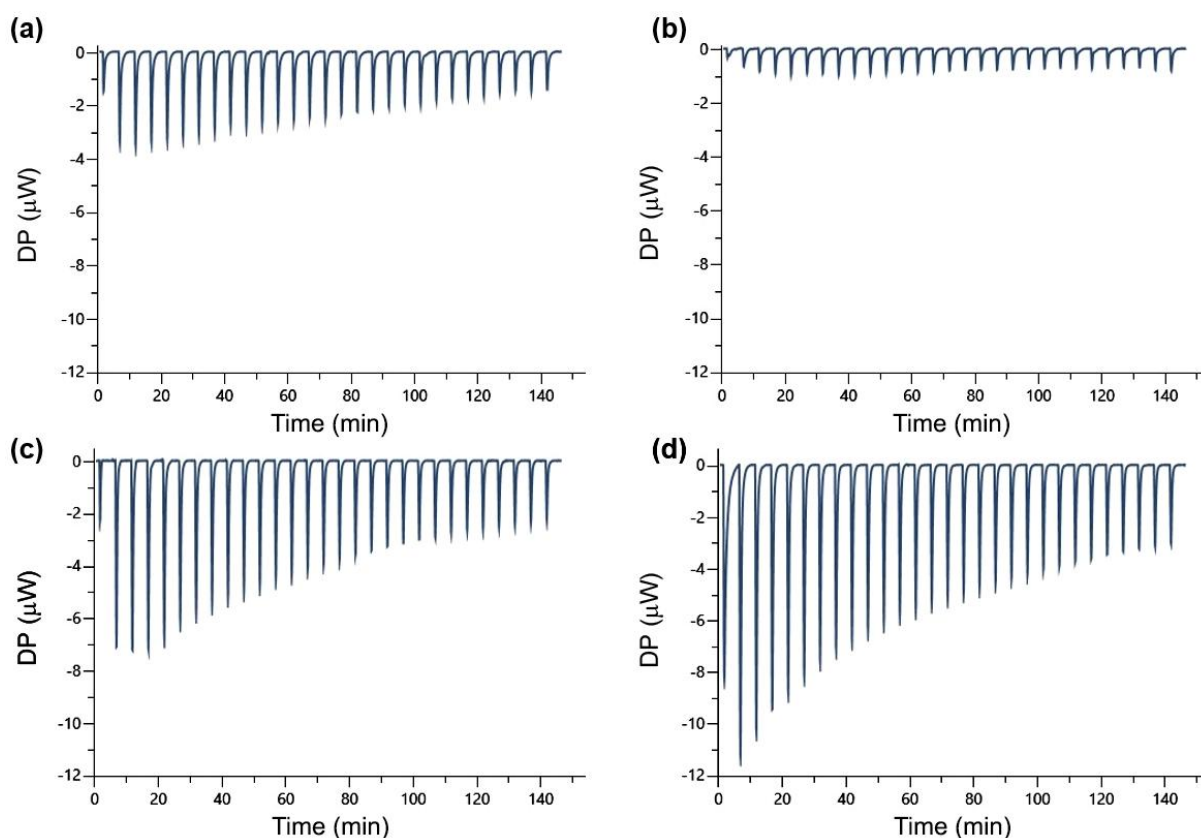


**Figure 5.** ITC thermograms obtained after injections of: (a) LecA onto **NP1-Gal** nanoparticles; (b) water with 100  $\mu\text{M}$   $\text{CaCl}_2$  onto **NP1-Gal** nanoparticles; (c) LecA onto **NP4-Glc** nanoparticles and (d) LecA onto **NP3-Gal** nanoparticles.

When the same experiment was performed with **NP4-Glc** nanoparticles, it surprisingly gave similar exothermic peaks (Figure 5c). Given the specificity of LecA for galactose, this unexpected result tends to confirm the existence of non-specific interactions in addition to carbohydrate-lectin interactions. They could be due to hydrophobic interactions from the high proportion of hydrophobic PCL-like sequences in the thioglycopolymers. They could lead to nonspecific binding of hydrophobic regions to LecA as reported previously,<sup>54</sup> to protein unfolding on nanoparticles surface or to non-specific H-bonds between glycosides and LecA. Also, protein-induced nanoparticle conformational change cannot be ruled out due to the lack of chemical cross-linking between the polymer chains. Moreover, since the thioglyconanoparticles are made of copolymers with statistical incorporation of glycosylated monomer units, only a small fraction (estimated to be ~15 %, see Supporting Information) is displayed on the surface of the nanoparticles, while most of them is located in their core, conversely to core-shell morphologies (e.g., glycosylated gold nanoparticles<sup>53</sup>), thus preventing LecA access to all galactose residues.

To improve the binding affinity of the thioglyconanoparticles for LecA, ITC experiments were first performed with **NP2-Gal** nanoparticles which contain 2-3 times more galactose residues per polymer chains than **NP1-Gal** nanoparticles, but without success since millimolar interactions ( $K_d \sim 3$  mM) were still obtained (see Figure S22). Conversely, increasing the length of the linker (i.e., from ethylene glycol to diethylene glycol) between the galactoside and the polymer backbone (**NP3-Gal**), resulted in a significant enhancement of the binding affinity, as shown by the nearly sigmoidal integration curve and the greatest exothermic signals obtained by ITC experiments (Figure 5d). For the evaluation of the dissociation constant, the thermogram of **NP4-Glc** was subtracted from the thermogram of **NP3-Gal** nanoparticles, since both copolymers have the same PCL-like backbone and we assumed that hydrophobic interactions between LecA and the backbone of **P4-Glc** were responsible for the exothermic peaks during the ITC experiment. Interestingly, the resulting analysis confirmed an interaction in the micromolar range ( $K_d \sim 5$   $\mu$ M), which is consistent with a carbohydrate-LecA interactions. These findings thus demonstrated the existence of specific carbohydrate-lectin interactions favored by the longer linker that promotes the accessibility of galactose moieties to lectins. Affinity in the micromolar range also highlighted the absence of a cluster glycoside effect,<sup>55</sup> as would be expected from polysaccharides or other multivalent glycoclusters that typically exhibit interactions in the nanomolar range.

### 3.5. Enzymatic degradation

Enzymatic degradation of the thioglyconanoparticles was investigated with Lipase B from *C. antarctica*, which is a widely used enzyme for the degradation of aliphatic polyesters and CKA-containing copolymers.<sup>37, 56-59</sup> After incubation of **NP1-Gal** nanoparticles with the enzyme for 24 h, the reaction mixture changed from a milky suspension of nanoparticles to a fully transparent solution with no visible insoluble deposits. SEC analyses showed a clear shift of the **P1-Gal** chromatogram toward very low molar masses when incubated with the enzyme whereas no decrease in  $M_n$  was noticed in its absence (Figure 6a). These results therefore support an enzymatic degradation mechanism of thioglycopolymers instead of a hydrolytic degradation mechanism. Upon degradation, the chromatogram of the degradation fragments overlapped with that of the enzyme- or salt-related byproducts which only gave an estimation of the  $M_n$  of the degradation products ( $M_n \sim 350 \text{ g}\cdot\text{mol}^{-1}$ ), which corresponds to a decrease in  $M_n$  above 90 %. The same result was obtained for **NP3-Gal** copolymers (Figure 6b).

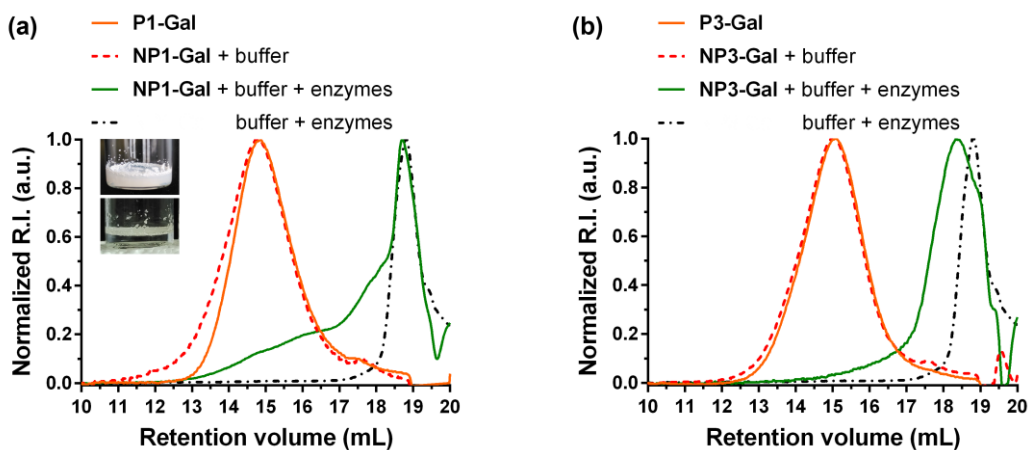


**Figure 6.** SEC chromatograms ( $\text{CHCl}_3/\text{TFA}$  0.1 vol.%) of: (a) **P1-Gal** copolymer (dashed red), **NP1-Gal** nanoparticles after incubation with (solid green) or without (solid orange) enzymes, and incubation of enzymes without nanoparticles (dashed-pointed black). Insert: Pictures of **NP1-Gal** nanoparticles at  $t = 0$  (top) and  $t = 1$  day (bottom) during enzymatic degradation with *C. antarctica*. (b) SEC chromatograms ( $\text{CHCl}_3/\text{TFA}$  0.1 vol.%) of the **P3-Gal** copolymer (dashed red), **NP3-Gal** nanoparticles after incubation with (solid green) or without (solid) enzymes, and incubation of enzymes without nanoparticles (dashed-pointed black) during enzymatic degradation with *C. antarctica*.

### 3.6. Biological evaluation

We first conducted preliminary cytocompatibility assays on two representative healthy cell lines (HUVEC and J774.A1), which would typically be exposed to nanoparticles after *in vivo* administration. **NP1-Gal** and **NP3-Gal** nanoparticles or their degradation products were tested at different concentrations, because neither the materials itself nor their degradation products should be cytotoxic when biomedical applications are envisioned. Cell viability was evaluated using the MTT mitochondrial reduction assay after a 72-h incubation period with the thioglyconanoparticles or their degradation products (Figure 7). On HUVEC cells, no significant cytotoxicity (> 75% cell viability) was observed up to 0.03 and 0.05 mg.mL<sup>-1</sup> for **NP1-Gal** and **NP3-Gal** nanoparticles, respectively, whereas on J774.A1 cells the concentrations reached 0.01 and 0.02 mg.mL<sup>-1</sup> for **NP1-Gal** and **NP3-Gal**, respectively. Also, when examining IC<sub>50</sub> values, **NP1-Gal** nanoparticles exhibited an IC<sub>50</sub> on J774.A1 cells of 0.03 mg.mL<sup>-1</sup>, which is ~3 fold higher than that of PCL-based nanoparticles after only a 24-h incubation period with the same cell line.<sup>60</sup> They also exhibited an IC<sub>50</sub> on HUVEC cells of 0.1 mg.mL<sup>-1</sup>, which is similar to PEGylated poly(alkyl cyanoacrylate) (PACA) nanoparticles after 24 h of incubation<sup>61</sup>. Interestingly, degradation products did not show significant decrease in cell viability up to at least 0.2 mg.mL<sup>-1</sup> for both thioglyconanoparticles on both cell lines, which makes these copolymers of promising interest for future biomedical uses.

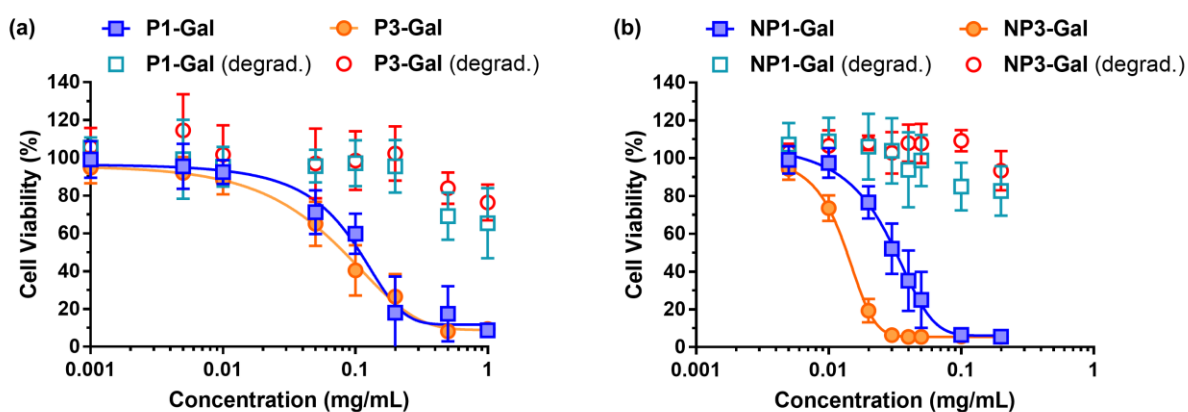


**Figure 7.** Cell viability (MTT assay) after incubation of: (a) HUVEC cells or (b) J774.A1 cells with increasing concentration of **NP1-Gal** nanoparticles and their degradation products and **NP3-Gal** nanoparticles and their degradation products. Results were expressed as percentages of absorption of treated cells ( $\pm$  SD) in comparison with the values obtained from untreated cells.

Fluorescent polymer nanoparticles are widely used as an imaging tool for theranostic applications.<sup>62</sup> To demonstrate the versatility of our new thioglycopolymers, we prepared fluorescent thioglycopolymer nanoparticles by the two main routes: (i) by physically encapsulating fluorescent molecules into the glyconanoparticles or (ii) by incorporating fluorescent moieties into the thioglycopolymer structure during its synthesis.

For the first strategy, a hydrophobic fluorophore, NR, was physically encapsulated in **NP1-Gal** nanoparticles during nanoprecipitation (Figure 8a). After THF evaporation, the resulting suspension of fluorescent nanoparticles was homogeneously purple without any insoluble precipitate (Figure 8b), whereas a heterogeneous mixture of insoluble pink solids in a faint pink supernatant was obtained in the absence of thioglycopolymers. Given the low-to-no solubility of NR in water ( $< 1 \mu\text{g}\cdot\text{mL}^{-1}$ ),<sup>63</sup> this result suggested the loading of NR into the thioglyconanoparticles. NR is also known to exhibit solvatochromic properties while its fluorescence is almost quenched in water.<sup>63</sup> While no UV absorption nor fluorescence emission has been measured for NR dispersed in water and for the non-fluorescent thioglyconanoparticles, NR-loaded **NP1-Gal** nanoparticles exhibited clear UV absorption ( $\lambda_{\text{max}} = 539 \text{ nm}$ ) and fluorescence emission ( $\lambda_{\text{em,max}} = 613 \text{ nm}$ ) spectra which supported the effective encapsulation inside the nanoparticle (Figure 8b and 8c). NR loading and encapsulation efficiency were determined to be 2 wt.% and 33 wt.% respectively after UV absorption of freeze-dried nanoparticles resolubilized in THF.

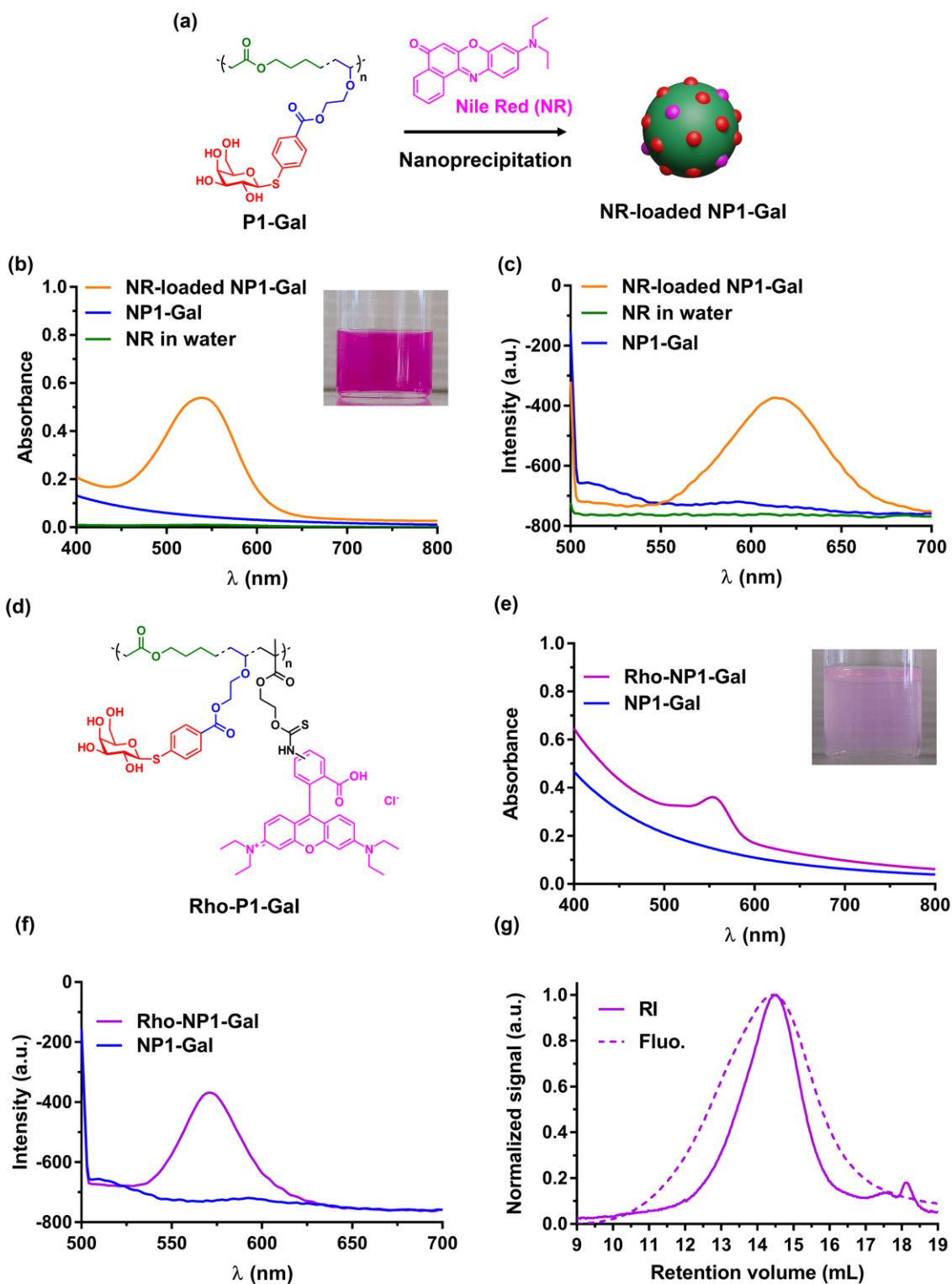


**Figure 8.** (a) Schematic representation of the formulation of NR-loaded **NP1-Gal** nanoparticles by nanoprecipitation. (b) UV absorption spectrum of NR-loaded **NP1-Gal** nanoparticles, **NP1-Gal** nanoparticles and NR solubilized in water. Insert: picture of NR-loaded **NP1-Gal** nanoparticles. (c) Fluorescence spectrum of NR-loaded **NP1-Gal** nanoparticles, **NP1-Gal** nanoparticles and NR solubilized in water. (d) Structure of **Rho-P1-Gal**. (e) UV absorption spectrum of **Rho-NP1-Gal** and **NP1-Gal**. Insert: picture of **Rho-NP1-Gal**. (f) Fluorescence spectrum of **Rho-NP1-Gal** and **NP1-Gal**. (g) SEC chromatogram (CHCl<sub>3</sub>/TFA 0.1 vol.%) of **Rho-P1-Gal**.

Fluorescent moieties were inserted into the thioglycopolymer structure via terpolymerization of 0.1 mol % methacryloxyethyl thiocarbamoyl Rhodamine B(RhoMA) with MDO and protected (AcO)<sub>4</sub>GalVE under the “*grafting through*” approach. After deprotection and purification, SEC and <sup>1</sup>H NMR analyses confirmed the formation of a P(MDO-*co*-GalVE-*co*-RhoMA) (**Rho-P1-Gal**, Figure 8d) terpolymer ( $M_n = 14\,000\text{ g}\cdot\text{mol}^{-1}$ ,  $\mathcal{D} = 1.5$ , Figure S23-25) with  $F_{VE} = 0.05$ . It was then formulated by nanoprecipitation into narrowly dispersed galactose-functionalized fluorescent **Rho-NP1-Gal** nanoparticles ( $D_z = 111$ , PSD = 0.1). Although the very low amount of RhoMA involved prevented the detection of proton signals related to Rhodamine B by <sup>1</sup>H NMR, the resulting terpolymer and **Rho-NP1-Gal** nanoparticles exhibited the intense pink color and fluorescence characteristic of Rhodamine B whereas Rhodamine B-free **NP1-Gal** exhibited none of these properties (Figure 8e and 8f). SEC confirmed a fluorescent response of the whole copolymer distribution (Figure 8e), thus supporting successful incorporation of RhoMA units in the terpolymer structure. Glucose-functionalized fluorescent thioglycopolymers (**Rho-P4-Glc**,  $M_n = 10\,100\text{ g}\cdot\text{mol}^{-1}$ ,  $\mathcal{D} = 1.9$ , figure S26-29) and the associated **Rho-NP4-Glc** nanoparticles ( $D_z = 102\text{ nm}$ , PSD = 0.07) were obtained under the same experimental conditions.

The cellular uptake of these fluorescent thioglyconanoparticles was then investigated by confocal microscopy experiment with human lung cancer cells (A549). We chose **Rho-NP1-Gal** and **Rho-NP4-Glc** thioglyconanoparticles instead of NR-loaded thioglyconanoparticles to avoid potential leakage of NR from the thioglyconanoparticles and thus more accurate confocal microscopy observations. After incubation of A549 cells with **Rho-NP1-Gal** and **Rho-NP4-Glc** nanoparticles, cells were labeled with calcein-AM, a well-known viability cell dye, prior to confocal microscopy observation in the median plane of cells (Figure 9). After 20 min of incubation, a few well-defined red spots appeared mainly at the periphery of the cells for both types of nanoparticles, whereas significant cell internalization of the nanoparticles was witnessed after 2 h of incubation. Note that a significant fraction of nanoparticles was still present at the cell surface, suggesting an ongoing internalization process. In conclusion, both **Rho-NP1-Gal** and **Rho-NP4-Glc** nanoparticles were able to be internalized by A549 cancer cells, which suggest potential use of these degradable thioglycopolymers in drug delivery and/or imaging applications.

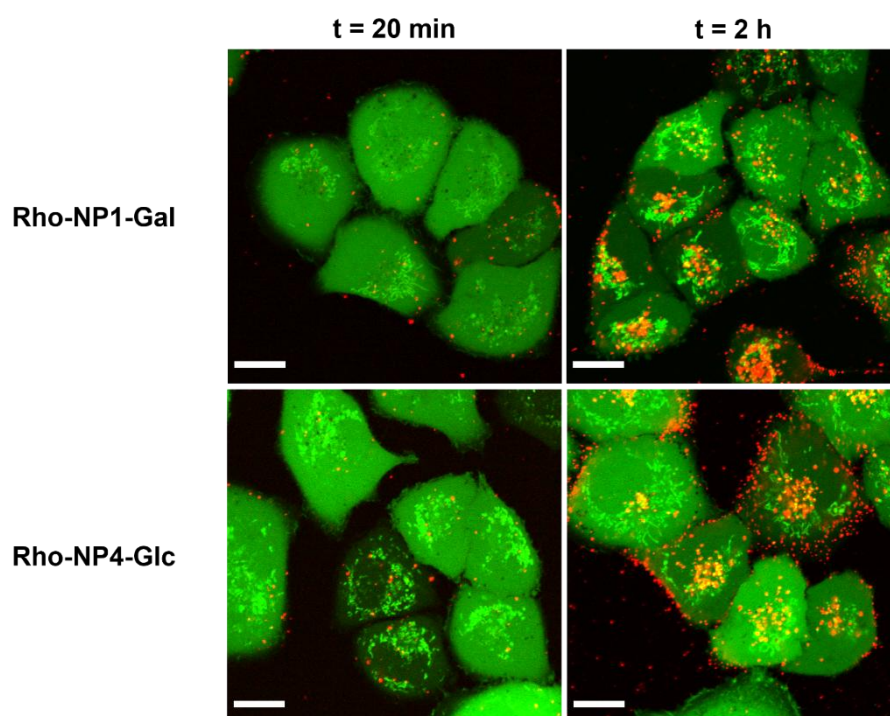


**Figure 9.** Merged fluorescence signals from the green (calcein) and red (rhodamine B) channels by confocal microscopy taken from the median plane of A549 cells after incubation with **Rho-NP1-Gal** (top row) or **Rho-NP4-Glc** (bottom row) for 20 min (left column) and 2 h (right column). Pictures were taken from median plane of cells. Scale bar = 10  $\mu\text{m}$ .

#### 4. Conclusion

In the present study, we reported the synthesis of degradable thioglycosylated polyester-like copolymers by rROP. A small library of P(MDO-co-VE) thioglycopolymers with tunable compositions and properties (e.g., fraction of VE units, length of the linker and nature of the thiosugar) was easily obtained following two different synthetic routes: the “grafting through” and the “grafting to” approaches. The thioglycopolymers were then formulated into stable and narrowly dispersed thioglyconanoparticles with or without surfactants, which exhibited enzymatic degradation and promising cytocompatibility when compared to well-established biodegradable polymers such as PCL or PACA. The thioglyconanoparticles also exhibited interactions with the lectin LecA. Even though ITC experiments suggested the existence of non-specific hydrophobic interactions between the thioglyconanoparticles and LecA, those were surpassed by optimization of the thioglycopolymer structure, especially by the introduction of a diethylene glycol linker between the thioglycoside and the copolymer backbone. Finally, fluorescent glyconanoparticles were successfully prepared, either by encapsulation of NR during formulation of the thioglycopolymers, or by grafting of Rhodamine B

moieties during the synthesis of the thioglycopolymers. The fluorescence labeling allowed us to follow the fate the thioglyconanoparticles, in particular, their significant internalization by A549 cancer cells. This comprehensive study demonstrated that P(MDO-co-VE) copolymers represent a robust and versatile platform to prepare polyester-like thioglycopolymers which met the key needs for potential drug delivery applications.

## Supporting Information

<sup>1</sup>H NMR spectra, SEC chromatograms, estimation of the fraction of glycoside residues on the surface of nanoparticles, ITC thermograms. This information is available free of charge via the Internet at <http://pubs.acs.org/>.

## Acknowledgments

We thank the ANR NanoCardioROP (ANR-15-CE08-0019) and the French Ministry of Research, respectively for the financial support of the Master 2 internship and the PhD thesis of TP. AI and EG acknowledge support from Glyco@Alps (ANR-15-IDEX-02) and Labex Arcane/CBH- EUR-GS (ANR-17-EURE-0003). Valérie Nicolas (UMS IPSIT, Univ Paris-Saclay) and Stéphanie Denis (IGPS, Univ Paris-Saclay) are acknowledged for her technical assistance in confocal microscopy and cell culture, respectively. Dr Johanna Tran is acknowledged for fruitful discussions.

## References

1. Sharon, N.; Lis, H., Carbohydrates in cell recognition. *Sci. Am.* **1993**, *268* (1), 82-89.
2. Winzler, R. J., Carbohydrates in cell surfaces. *Int. Rev. Cytol.* **1970**, *29*, 77-125.
3. Brandley, B. K.; Schnaar, R. L., Cell-surface carbohydrates in cell recognition and response. *J. Leukoc. Biol.* **1986**, *40* (1), 97-111.
4. Dabelsteen, E., Cell surface carbohydrates as prognostic markers in human carcinomas. *J. Pathol.* **1996**, *179* (4), 358-369.
5. Pieters, R. J., Carbohydrate Mediated Bacterial Adhesion. In *Bacterial Adhesion: Chemistry, Biology and Physics*, Linke, D.; Goldman, A., Eds. Springer Netherlands: Dordrecht, 2011; pp 227-240.
6. Ofek, I.; Kahane, I.; Sharon, N., Toward anti-adhesion therapy for microbial diseases. *Trends Microbiol.* **1996**, *4* (8), 297-299.
7. Hansen, J.-E.; Nielsen, C. M.; Nielsen, C.; Heegaard, P.; Mathiesen, L.; Nielsen, J., Correlation between carbohydrate structures on the envelope glycoprotein gp120 of HIV-1 and HIV-2 and syncytium inhibition with lectins. *AIDS* **1989**, *3* (10), 635-641.

8. Kamali, A.; Holodniy, M., Influenza treatment and prophylaxis with neuraminidase inhibitors: a review. *Infect. Drug. Resist.* **2013**, *6*, 187.
9. Lackenby, A.; Thompson, C. I.; Democratis, J., The potential impact of neuraminidase inhibitor resistant influenza. *Curr. Opin. Infect. Dis.* **2008**, *21* (6), 626-638.
10. Pantophlet, R.; Burton, D. R., GP120: target for neutralizing HIV-1 antibodies. *Annu. Rev. Immunol.* **2006**, *24*, 739-769.
11. Suarez, D. L.; Schultz-Cherry, S., Immunology of avian influenza virus: a review. *Dev. Comp. Immunol.* **2000**, *24* (2-3), 269-283.
12. Montoir, D.; Amoura, M.; Ababsa, Z. E. A.; Vishwanatha, T.; Yen-Pon, E.; Robert, V.; Beltramo, M.; Piller, V.; Alami, M.; Aucagne, V., Synthesis of aryl-thioglycopeptides through chemoselective Pd-mediated conjugation. *Chem. Sci.* **2018**, *9* (46), 8753-8759.
13. Gim, S.; Zhu, Y.; Seeberger, P. H.; Delbianco, M., Carbohydrate-based nanomaterials for biomedical applications. *Wiley Interdiscip. Rev.: Nanomed. Nanobiotechnology* **2019**, *11* (5), e1558.
14. Lemarchand, C.; Gref, R.; Couvreur, P., Polysaccharide-decorated nanoparticles. *Eur. J. Pharm. Biopharm.* **2004**, *58* (2), 327-341.
15. Liu, Z.; Jiao, Y.; Wang, Y.; Zhou, C.; Zhang, Z., Polysaccharides-based nanoparticles as drug delivery systems. *Adv. Drug Del. Rev.* **2008**, *60* (15), 1650-1662.
16. Kottari, N.; Chabre, Y. M.; Sharma, R.; Roy, R., Applications of Glyconanoparticles as "Sweet" Glycobiological Therapeutics and Diagnostics. In *Multifaceted Development and Application of Biopolymers for Biology, Biomedicine and Nanotechnology*, Dutta, P. K.; Dutta, J., Eds. Springer Berlin Heidelberg: Berlin, Heidelberg, 2013; pp 297-341.
17. Solá, R. J.; Griebenow, K., Effects of glycosylation on the stability of protein pharmaceuticals. *J. Pharm. Sci.* **2009**, *98* (4), 1223-1245.
18. Solá, R. J.; Griebenow, K., Glycosylation of therapeutic proteins. *Biodrugs* **2010**, *24* (1), 9-21.
19. Novartis Sandostatin LAR Depot (Octreotide Acetate for Injectable Suspension). [https://www.novartis.us/sites/www.novartis.us/files/sandostatin\\_lar.pdf](https://www.novartis.us/sites/www.novartis.us/files/sandostatin_lar.pdf) (visited on 12/4/2022)
20. Li, X.; Chen, G., Glycopolymer-based nanoparticles: synthesis and application. *Polym. Chem.* **2015**, *6* (9), 1417-1430.
21. Pelegri-O'Day, E. M.; Paluck, S. J.; Maynard, H. D., Substituted polyesters by thiol-ene modification: Rapid diversification for therapeutic protein stabilization. *J. Am. Chem. Soc.* **2017**, *139* (3), 1145-1154.
22. Pelegri-O'Day, E. M.; Bhattacharya, A.; Theopold, N.; Ko, J. H.; Maynard, H. D., Synthesis of zwitterionic and trehalose polymers with variable degradation rates and stabilization of insulin. *Biomacromolecules* **2020**, *21* (6), 2147-2154.
23. Krannig, K.-S.; Doriti, A.; Schlaad, H., Facilitated synthesis of heterofunctional glycopolypeptides. *Macromolecules* **2014**, *47* (7), 2536-2539.
24. Tao, Y.; He, J.; Zhang, M.; Hao, Y.; Liu, J.; Ni, P., Galactosylated biodegradable poly ( $\epsilon$ -caprolactone-co-phosphoester) random copolymer nanoparticles for potent hepatoma-targeting delivery of doxorubicin. *Polym. Chem.* **2014**, *5* (10), 3443-3452.
25. Pramudya, I.; Chung, H., Recent progress of glycopolymer synthesis for biomedical applications. *Biomater. Sci.* **2019**, *7* (12), 4848-4872.
26. Lecomte, P.; Jérôme, C., Recent Developments in Ring-Opening Polymerization of Lactones. In *Synthetic Biodegradable Polymers*, Rieger, B.; Künkel, A.; Coates, G. W.; Reichardt, R.; Dinjus, E.; Zevaco, T. A., Eds. Springer Berlin Heidelberg: Berlin, Heidelberg, 2012; pp 173-217.
27. Corrigan, N.; Jung, K.; Moad, G.; Hawker, C. J.; Matyjaszewski, K.; Boyer, C., Reversible-deactivation radical polymerization (Controlled/living radical polymerization): From discovery to materials design and applications. *Prog. Polym. Sci.* **2020**, *111*, 101311.
28. Aliferis, T.; Iatrou, H.; Hadjichristidis, N., Living polypeptides. *Biomacromolecules* **2004**, *5* (5), 1653-1656.

29. Dubois, P.; Coulembier, O.; Raquez, J.-M., *Handbook of ring-opening polymerization*. John Wiley & Sons: 2009.
30. Miura, Y.; Hoshino, Y.; Seto, H., Glycopolymer nanobiotechnology. *Chem. Rev.* **2016**, *116* (4), 1673-1692.
31. Tardy, A.; Nicolas, J.; Gimes, D.; Lefay, C.; Guillaneuf, Y., Radical ring-opening polymerization: Scope, limitations, and application to (bio) degradable materials. *Chem. Rev.* **2017**, *117* (3), 1319-1406.
32. Pesenti, T.; Nicolas, J., 100th Anniversary of Macromolecular Science Viewpoint: Degradable Polymers from Radical Ring-Opening Polymerization: Latest Advances, New Directions, and Ongoing Challenges. *ACS Macro Lett.* **2020**, *9*, 1812-1835.
33. Jackson, A. W., Reversible-deactivation radical polymerization of cyclic ketene acetals. *Polym. Chem.* **2020**, *11* (21), 3525-3545.
34. Xiao, N.; Zhong, L.; Zhai, W.; Bai, W., Preparation of well-defined and degradable aldehyde-functionalized glycopolymeric nanospheres. *Acta Polym. Sin.* **2012**, *8*, 818-824.
35. Lau, U. Y.; Pelegri-O'Day, E. M.; Maynard, H. D., Synthesis and biological evaluation of a degradable trehalose glycopolymer prepared by RAFT polymerization. *Macromol. Rapid Commun.* **2018**, *39* (5), 1700652.
36. Ganda, S.; Jiang, Y.; Thomas, D. S.; Eliezar, J.; Stenzel, M. H., Biodegradable glycopolymeric micelles obtained by RAFT-controlled radical ring-opening polymerization. *Macromolecules* **2016**, *49* (11), 4136-4146.
37. Tran, J.; Pesenti, T.; Cressonnier, J.; Lefay, C.; Gimes, D.; Guillaneuf, Y.; Nicolas, J., Degradable copolymer nanoparticles from radical ring-opening copolymerization between cyclic ketene acetals and vinyl ethers. *Biomacromolecules* **2018**, *20* (1), 305-317.
38. Tardy, A.; Honoré, J. C.; Tran, J.; Siri, D.; Delplace, V.; Bataille, I.; Letourneur, D.; Perrier, J.; Nicoletti, C.; Maresca, M., Radical copolymerization of vinyl ethers and cyclic ketene acetals as a versatile platform to design functional polyesters. *Angew. Chem.* **2017**, *129* (52), 16742-16747.
39. Bruneau, A.; Roche, M.; Hamze, A.; Brion, J. D.; Alami, M.; Messaoudi, S., Stereoretentive Palladium-Catalyzed Arylation, Alkenylation, and Alkynylation of 1-Thiosugars and Thiols Using Aminobiphenyl Palladacycle Precatalyst at Room Temperature. *Chem. Eur. J.* **2015**, *21* (23), 8375-8379.
40. Gilboa-Garber, N., [32] Pseudomonas aeruginosa lectins. In *Methods Enzymol.*, Elsevier: 1982; Vol. 83, pp 378-385.
41. Cioci, G.; Mitchell, E. P.; Gautier, C.; Wimmerová, M.; Sudakevitz, D.; Pérez, S.; Gilboa-Garber, N.; Imberty, A., Structural basis of calcium and galactose recognition by the lectin PA-IL of Pseudomonas aeruginosa. *FEBS Lett.* **2003**, *555* (2), 297-301.
42. Blanchard, B.; Nurisso, A.; Hollville, E.; Tetaud, C.; Wiels, J.; Pokorná, M.; Wimmerová, M.; Varrot, A.; Imberty, A., Structural basis of the preferential binding for globo-series glycosphingolipids displayed by Pseudomonas aeruginosa lectin I. *J. Mol. Biol.* **2008**, *383* (4), 837-853.
43. Tran, J.; Guégain, E.; Ibrahim, N.; Harrisson, S.; Nicolas, J., Efficient synthesis of 2-methylene-4-phenyl-1, 3-dioxolane, a cyclic ketene acetal for controlling the NMP of methyl methacrylate and conferring tunable degradability. *Polym. Chem.* **2016**, *7* (26), 4427-4435.
44. Vinogradova, E. V.; Zhang, C.; Spokoyny, A. M.; Pentelute, B. L.; Buchwald, S. L., Organometallic palladium reagents for cysteine bioconjugation. *Nature* **2015**, *526* (7575), 687-691.
45. Probst, N.; Lartia, R.; Théry, O.; Alami, M.; Defrancq, E.; Messaoudi, S., Efficient Buchwald–Hartwig–Migita Cross-Coupling for DNA Thioglycoconjugation. *Chem. Eur. J.* **2018**, *24* (8), 1795-1800.
46. Chu, X.; Shen, L.; Li, B.; Yang, P.; Du, C.; Wang, X.; He, G.; Messaoudi, S.; Chen, G., Construction of peptide macrocycles via palladium-catalyzed multiple S-arylation: an effective strategy to expand the structural diversity of cross-linkers. *Org. Lett.* **2021**, *23* (20), 8001-8006.

47. Garber, N.; Guempel, U.; Belz, A.; Gilboa-Garber, N.; Doyle, R. J., On the specificity of the D-galactose-binding lectin (PA-I) of *Pseudomonas aeruginosa* and its strong binding to hydrophobic derivatives of D-galactose and thiogalactose. *Biochim. Biophys. Acta - Gen. Subj.* **1992**, *1116* (3), 331-333.
48. Kadam, R. U.; Garg, D.; Schwartz, J.; Visini, R.; Sattler, M.; Stocker, A.; Darbre, T.; Reymond, J.-L., CH- $\pi$  "T-Shape" Interaction with Histidine Explains Binding of Aromatic Galactosides to *Pseudomonas aeruginosa* Lectin LecA. *ACS Chem. Biol.* **2013**, *8* (9), 1925-1930.
49. Rodrigue, J.; Ganne, G.; Blanchard, B.; Saucier, C.; Giguère, D.; Shiao, T. C.; Varrot, A.; Imberty, A.; Roy, R., Aromatic thioglycoside inhibitors against the virulence factor LecA from *Pseudomonas aeruginosa*. *Org. Biomol. Chem.* **2013**, *11* (40), 6906-6918.
50. Dong, C. M.; Faucher, K. M.; Chaikof, E. L., Synthesis and properties of biomimetic poly (l-glutamate)-b-poly (2-acryloyloxyethyl lactoside)-b-poly (l-glutamate) triblock copolymers. *J. Polym. Sci., Part A: Polym. Chem.* **2004**, *42* (22), 5754-5765.
51. Zhao, Y.; Lu, Z.; Dai, X.; Wei, X.; Yu, Y.; Chen, X.; Zhang, X.; Li, C., Glycomimetic-conjugated photosensitizer for specific *Pseudomonas aeruginosa* recognition and targeted photodynamic therapy. *Bioconj. Chem.* **2018**, *29* (9), 3222-3230.
52. Harrowven, D. C.; Nunn, M. I.; Newman, N. A.; Fenwick, D. R., A new cascade radical reaction for the synthesis of biaryls and triaryls from benzyl iodoaryl ethers. *Tetrahedron Lett.* **2001**, *42* (5), 961-964.
53. Reynolds, M.; Marradi, M.; Imberty, A.; Penadés, S.; Pérez, S., Multivalent gold glycoclusters: high affinity molecular recognition by bacterial lectin PA-IL. *Chem. Eur. J.* **2012**, *18* (14), 4264-4273.
54. Stoitsova, S. R.; Boteva, R. N.; Doyle, R., Binding of hydrophobic ligands by *Pseudomonas aeruginosa* PA-I lectin. *Biochim. Biophys. Acta - Gen. Subj.* **2003**, *1619* (2), 213-219.
55. Cecioni, S.; Imberty, A.; Vidal, S., Glycomimetics versus multivalent glycoconjugates for the design of high affinity lectin ligands. *Chem. Rev.* **2015**, *115* (1), 525-561.
56. Hedir, G. G.; Arno, M. C.; Langlais, M.; Husband, J. T.; O'Reilly, R. K.; Dove, A. P., Poly (oligo (ethylene glycol) vinyl acetate) s: A Versatile Class of Thermoresponsive and Biocompatible Polymers. *Angew. Chem.* **2017**, *129* (31), 9306-9310.
57. Kundys, A.; Białecka-Florjańczyk, E.; Fabiszewska, A.; Małajowicz, J., *Candida antarctica* lipase B as catalyst for cyclic esters synthesis, their polymerization and degradation of aliphatic polyesters. *J. Polym. Environ.* **2018**, *26* (1), 396-407.
58. Guégain, E.; Michel, J.-P.; Boissenot, T.; Nicolas, J., Tunable degradation of copolymers prepared by nitroxide-mediated radical ring-opening polymerization and point-by-point comparison with traditional polyesters. *Macromolecules* **2018**, *51* (3), 724-736.
59. Lutz, J.-F.; Andrieu, J.; Üzgün, S.; Rudolph, C.; Agarwal, S., Biocompatible, thermoresponsive, and biodegradable: simple preparation of "all-in-one" biorelevant polymers. *Macromolecules* **2007**, *40* (24), 8540-8543.
60. Lemarchand, C.; Gref, R.; Passirani, C.; Garcion, E.; Petri, B.; Müller, R.; Costantini, D.; Couvreur, P., Influence of polysaccharide coating on the interactions of nanoparticles with biological systems. *Biomaterials* **2006**, *27* (1), 108-118.
61. Orlando, A.; Re, F.; Sesana, S.; Rivolta, I.; Panariti, A.; Brambilla, D.; Nicolas, J.; Couvreur, P.; Andrieux, K.; Masserini, M., Effect of nanoparticles binding  $\beta$ -amyloid peptide on nitric oxide production by cultured endothelial cells and macrophages. *Int. J. Nanomedicine* **2013**, *8*, 1335.
62. Indoria, S.; Singh, V.; Hsieh, M.-F., Recent advances in theranostic polymeric nanoparticles for cancer treatment: A review. *Int. J. Pharm.* **2020**, *582*, 119314.
63. Greenspan, P.; Fowler, S. D., Spectrofluorometric studies of the lipid probe, Nile red. *J. Lipid Res.* **1985**, *26* (7), 781-789.

## Graphical abstract

